AECL-9714

ATOMIC ENERGY OF CANADA LIMITED

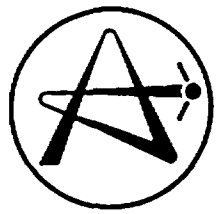

ÉNERGIE ATOMIQUE DU CANADA LIMITÉE

DETECTING, LOCATING AND IDENTIFYING FAILED FUEL IN CANADIAN POWER REACTORS

DÉTECTION, LOCALISATION ET IDENTIFICATION DE LA GAINE DE COMBUSTIBLE ROMPUE DES RÉACTEURS DE PUISSANCE CANADIENS

R.D. MacDONALD, M.R. FLOYD, B.J. LEWIS, A.M. MANZER AND P.T. TRUANT

Prepared for the IAEA Coordinated Research Program on the
Examination and Documentation Methodology for Water Reactor Fuel (ED-WARF)

Chalk River Nuclear Laboratories
Laboratoires nucléaires de Chalk River

Chalk River, Ontario K0J 1J0

February 1990 février

ATOMIC ENERGY OF CANADA LIMITED

DETECTING, LOCATING AND IDENTIFYING FAILED FUEL IN CANADIAN POWER REACTORS

by

R.D. MacDonald, M.R. Floyd*, B.J. Lewis+, A.M. Manzer**, and P.T. Truant*

Prepared for the IAEA Coordinated Research Program on the Examination and Documentation Methodology for Water Reactor Fuel (ED-WARF)

* Ontario Hydro, Central Nuclear Services, 700 University Avenue, Toronto, Ontario, M5G 1X6

** AECL CANDU Operations, 2251 Speakman Drive, Mississauga, Ontario, L5K 1B2

+ Department of Chemistry and Chemical Engineering, Royal Military College, Kingston, Ontario, K7K 5L0

Fuel Engineering Branch
Chalk River Nuclear Laboratories
Chalk River, Ontario K0J 1J0
1990 February

AECL-9714

ÉNERGIE ATOMIQUE DU CANADA LIMITÉE

DÉTECTION, LOCALISATION ET IDENTIFICATION DE LA GAINE DE COMBUSTIBLE ROMPUE DES RÉACTEURS DE PUISSANCE CANADIENS

par

R.D. MacDonald, M.R. FLoyd*, B.J. Lewis+, A.M. Manzer**
et P.T. Truant*

Rédigé pour le Programme de recherche coordonné de L'AIEA sur les méthodes d'Examen et de Documentation du Combustible de Réacteurs à Eau (ED-CRE) (ED-WARF)

RÉSUMÉ

Ce document résume les moyens de détecter, de localiser et d'identifier les éléments de combustible rendu défectueux dans les réacteurs de puissance CANDU canadiens. On détecte les défauts du combustible en surveillant le caloporteur primaire quant aux produits de fission gazeux et aux radioiodes tandis qu'on les localise habituellement dans le coeur, en cours de marche, en surveillant les échantillons de caloporteur provenant des canaux de combustible particuliers ou en cours d'arrêt en surveillant les tuyaux d'alimentation des canaux quant aux rayons gamma. Les systèmes et techniques servant à détecter et localiser le combustible rendu défectueux dans les centrales d'Ontario Hydro et CANDU-6, y sont décrits ainsi que des exemples fournis par l'expérience avec les centrales. Les possibilités de détection et localisation du combustible rendu défectueux dans les centrales sont beaucoup plus grandes avec un programme de RD fondamentaux ayant permis de mieux comprendre des modèles de libération et migration des produits de fission et détérioration postérieure par défectuosité de la gaine de combustible rompue. Les techniques et le matériel servant à identifier et stocker le combustible rendu défectueux après son déchargement du réacteur y sont examinés brièvement.

* Ontario Hydro, Services nucléaires centraux, 700 University Avenue, Toronto, Ontario, M5G 1X6

** EACL, Opérations CANDU, 2251 Speakman Drive, Mississauga, Ontario, L5K 1B2

+ Département de Chimie et génie chimique, Collège Militaire Royal, Kingston, Ontario, K7K 5L0

Génie des combustibles
Laboratoires nucléaires de Chalk River
Chalk River, Ontario K0J 1J0
1990 février

AECL-9714

ATOMIC ENERGY OF CANADA LIMITED

DETECTING, LOCATING AND IDENTIFYING FAILED FUEL IN CANADIAN POWER REACTORS

by

R.D. MacDonald, M.R. Floyd*, B.J. Lewis+, A.M. Manzer**, and P.T. Truant*

Prepared for the IAEA Coordinated Research Program on the Examination and Documentation Methodology for Water Reactor Fuel (ED-WARF)

ABSTRACT

This document summarizes how defected fuel elements are detected, located and identified in Canadian CANDU power reactors. Fuel defects are detected by monitoring the primary coolant for gaseous fission products and radioiodines, while location in core is usually performed on-power by delayed neutron monitoring of coolant samples from individual fuel channels or off-power by gamma-ray monitoring of the channel feeder pipes. The systems and techniques used to detect and locate defected fuel in both Ontario Hydro and CANDU 6 power stations are described, along with examples provided by station experience. The ability to detect and locate defected fuel in power stations was greatly enhanced by a fundamental R&D program, which provided an understanding and models of fission-product release and transport, and the post-defect deterioration of failed fuel. Techniques and equipment used to identify and store defected fuel after it has been discharged from the reactor are briefly reviewed.

* Ontario Hydro, Central Nuclear Services, 700 University Avenue, Toronto, Ontario, M5G 1X6

** AECL CANDU Operations, 2251 Speakman Drive, Mississauga, Ontario, L5K 1B2

+ Department of Chemistry and Chemical Engineering, Royal Military College, Kingston, Ontario, K7K 5L0

Fuel Engineering Branch
Chalk River Nuclear Laboratories
Chalk River, Ontario K0J 1J0
1990 February

AECL-9714

A. INTRODUCTION

The CANDU* pressurized heavy water (PHW) reactor is a pressure-tube design which uses heavy water (D_2O) as both the moderator and coolant. The reactor is fuelled with 500 mm long fuel bundles of natural uranium dioxide clad in Zircaloy-4 sheathing. These bundles can be inserted and removed on-power from the pressure tubes of all fuel channels. Two types of fuel bundles are commonly used in Canadian CANDU-PHW reactors: a bundle consisting of 28 fuel elements (Pickering Nuclear Generating Station (NGS)) and 37-element bundle (Bruce and CANDU 6 (NGS)). The 28-element bundles have elements with a slightly larger diameter than those in the 37-element bundle, although both have comparable element linear powers. Figure 1 shows the element and bundle parameters for both types of Canadian CANDU-PHW fuel. Because our fuel is natural UO_2 and the bundles are inexpensive to manufacture, CANDU reactors operate on a once-through fuel cycle. For these same reasons, reconstitution of bundles with defected elements is not necessary or practised in CANDU power stations.

Each of the horizontal fuel channels in a CANDU reactor contains twelve bundles within the reactor core. The on-power refuelling system of a CANDU uses two remotely operated fuelling machines, one at each end of the channel. During refuelling, the machines operate in pairs, locking onto opposite ends of the same channel. One machine inserts new-fuel bundles into the channel, while the other accepts the same number of discharged bundles. The number of bundles replaced in a channel during refuelling depends on the fuel-management scheme used by the utility; the most common number of bundles shifted during refuelling are 2, 4, 8 and 10.

Fuel performance in Canadian CANDU reactors has been excellent; 99.9% of more than 550 000 fuel bundles irradiated to date have operated as designed. The cumulative defect rate for CANDU fuel is 0.1%, with the current rate running below 0.05% (1). The fuel defects that have occurred in Canadian reactors can be classified into four types:

(a) Stress-corrosion defects - stress-corrosion cracking (SCC) of the fuel-element sheath that can occur during power ramps, as a result of high stresses in the Zircaloy in the presence of fission products, notably iodine.

(b) Fabrication defects - flaws in the fuel elements induced during fabrication that can allow coolant to enter the elements. The most common flaws have been faulty end-plug welds and a few porous "piping" defects in the end-plug material.

*CANDU: CANada Deuterium Uranium. Registered trademark of Atomic Energy of Canada Limited.

(c) Fretting defects - small pieces of debris in the heat-transport circuit that can be trapped within the bundle and penetrate fuel-element sheaths by a fretting mechanism driven by the coolant flow.

(d) Circumferential cracking near end-cap welds - hydrogen (or deuterium) in the Zircaloy cladding can diffuse to areas of high stress and low temperature near the welds and cause cracking.

Current practice in fuel fabrication, design and operation has reduced fuel defects in Canadian CANDU reactors to extremely low levels. These measures include CANLUB coating on the inside of the sheath to prevent SCC, better quality control during manufacturing, and the inclusion of channel strainers during reactor commissioning to remove debris left over from construction.

Regardless of the defect mechanism, failed fuel in the reactor core can release radioiodines, gaseous and solid fission products and fuel debris into the coolant. The amounts released depend on such factors as fuel-element power, the time the defected fuel is in-core, the size of the initial defect and the deterioration rate of the failed fuel element. As a general principle, defected CANDU fuel is discharged from the core as soon as practical after it has been detected and located. Early detection and removal of defected fuel has contributed to clean heat-transport systems, thereby minimizing occupational radiation exposures to reactor operating staff. Low radiation exposure to personnel is a hallmark of CANDU reactors (2).

Because of on-power refuelling, the CANDU system is well suited for removing defected fuel without any reduction in reactor power. Once detected and located, the defected fuel can be discharged by the fuelling machines into the reactor's irradiated fuel bays. Purification circuits with ion-exchange columns are used to remove the radioiodines from the primary coolant.

In Canadian CANDU reactors, failed fuel is detected by monitoring the primary coolant for gaseous fission products and radioiodines. Defects in-core are located either by delayed neutron (DN) monitoring of coolant samples from individual fuel channels or by DN monitoring of the reactor feeder pipes. Table A summarizes the detection and location systems in Canadian CANDU reactors:

TABLE A

FUEL FAILURE DETECTION AND LOCATION SYSTEMS IN CANADIAN CANDU REACTORS

CANADIAN CANDU REACTORS	FAILED FUEL DETECTION	FAILED FUEL LOCATION
PICKERING A (4-unit station) 515 MWe net capacity each unit	Analyses by the station chemistry laboratory of the radioactivity in samples from the primary heat-transport system on a regular schedule	No system available
PICKERING B (4-unit station) 516 MWe net capacity each unit	Same as Pickering A	Scanning of outlet feeders off-power using standard Geiger tubes. Dry-sipping of all routinely discharged fuel.
BRUCE A (4-unit station) 825 MWe net capacity each unit	Coolant samples from the primary heat-transport system are analyzed for radioactivity on a regular schedule	Delayed neutron monitoring of individual channels on-power (performed when I-131 in the coolant is greater than 5 μCi/kg)
BRUCE B (4-unit station) 825 MWe net capacity each unit	Continuous on-line monitoring for Xe-133, Xe-135, Kr-88 and I-131 in the primary heat-transport system. Coolant samples are also analyzed for radioactivity on a regular schedule.	Fully automated monitoring of delayed neutron signals from individual channels on a regular schedule
DARLINGTON (4-unit station under construction) 881 MWe net capacity each unit	Same as Bruce B	Automatically operated feeder-scanner system using spectrum adjusted Geiger tubes designed to be used off-power
CANDU 6 (Pt. Lepreau and Gentilly-2) 638 MWe net capacity each unit	Same as Bruce B	Delayed neutron monitoring on-power performed weekly, bi-weekly or after transient release of noble gases and iodine

In the following sections we will summarize how defected fuel is detected, located and identified in Canadian CANDU reactors. Each of these three categories will be illustrated with examples from station operation. Because of the differences in the detection systems and the physical parameters of the reactors, our power station experience will be described in two separate sections, one for Ontario Hydro's Pickering and Bruce stations and the other for AECL-designed CANDU 6 stations, New Brunswick Power's Point Lepreau and Hydro-Quebec's Gentilly-2. The report opens with a section on our fundamental studies on fuel-defect behaviour, which includes our experimental work on single-element tests and the development of fuel-defect models. This fundamental program, centred at the Chalk River Nuclear Laboratories (CRNL), has provided an in-depth understanding of fission-product transport and release and of post-defect deterioration (3). This information has had a profound effect on how defected fuel is detected and located in CANDU power stations. The report concludes with a section briefly describing how defected fuel is inspected, handled and stored underwater in the irradiated fuel bays associated with each of our power stations.

In this document the term defected fuel refers to a fuel element where the cladding has been breached to allow sufficient fission-product release into the coolant to be detected by the reactor monitoring systems. Such fuel elements are termed to be failed. The defects can be either large primary defects due to operational problems (overpower, etc.) or secondary damage resulting from very small primary defects. Some fuel elements with tiny breaches in the clad do not release fission products in large enough quantities to be detected by reactor monitoring systems; these elements are termed to be defective. Only when secondary damage occurs and the clad breach is enlarged are these elements defected.

B. EXPERIMENTAL PROGRAM ON FUNDAMENTAL DEFECT BEHAVIOUR (B.J. Lewis)

An experimental program with defected CANDU-type UO_2 fuel elements was carried out at CRNL from 1975 to 1983. Failed elements with various degrees of sheath damage were irradiated in separate tests in an experimental loop of the NRX reactor. In this program, the irradiation history of the elements and the characteristics of the failures (i.e., the size and location of defects) were well known. A feature of this study was the absence of complications in activity analysis caused by such effects as fission-product release from tramp uranium*, and the operation of coolant cleanup systems.

The experiments themselves were designed to provide a large data base for assessing fission-product release and post-defect behaviour under a variety of irradiation conditions.

*Tramp uranium is the term used to define uranium contamination of the in-core portion of the primary heat-transport system.

A brief summary of the fuel-operating parameters for each experiment is given in Table 1, with details of the fuel-element design listed in Table 2. All experiments used fuel elements which were either artificially or naturally defective. Some fuel elements were defected prior to irradiation with drilled holes or machined slits in the fuel sheathing. Other elements were characteristic of "natural" failures found in the power plant, defected by either small manufacturing flaws induced during fuel fabrication, or through stress-induced cracking of the fuel sheathing following a power ramp. The naturally-failed fuel was particularly susceptible to the phenomenon of sheath hydriding, with the hydride process leading to further deterioration of the sheath. As these experiments demonstrated, there is a critical primary defect size above which sheath hydriding did not occur, because the ratio of oxygen to hydrogen is sufficiently high that a protective oxide film is formed or maintained on the inside surface of the sheath (4,5).

On the basis of these experiments, a model was developed to describe the release of radioactive iodine and noble gas from defected fuel into the primary coolant. The model details the fission-product release behaviour for both a reactor operating at constant power, and for the transient condition of a reactor shutdown. An analytical treatment was also developed for the low-temperature release of fission products from small particles of fuel deposited on the in-core surfaces of the heat-transport system.

A methodology is illustrated that distinguishes between the activity released from fuel failures, and that from fuel debris or uranium contamination deposited on in-core surfaces. Once these two sources of fission-product release are identified, the condition of the reactor core can be quantitatively characterized in terms of the average size of defect, the number of fuel failures, and the amount of in-core uranium contamination.

B.1 The Experimental Facility and Monitoring Systems

The X-2 defect loop facility, shown in Figure 2, operates at the coolant conditions specified for CANDU power reactors. Details of the loop operational parameters are given in Table 3. This loop is designed to cope with high-activity levels caused by fission-product release and fuel loss through large defects. The full-flow graphite filters of the loop trap large grains of UO_2 fuel. Separate side-stream circuits for the ion-exchange mixed-bed resin columns and the degassing system provide an optional coolant-cleanup capability for both radioiodines and noble gases.

Activity releases to the coolant were monitored continuously with on-line gamma-ray spectrometry. Each spectrometer (see Figure 2) employs an intrinsic germanium detector with a resolution of better than 2 keV (FWHM) at 122 keV. The count rate for the detector was kept within specified limits by using various levels of attenuation provided by different-sized collimators. At the inlet to the reactor test section (monitoring zone M1), a spectrometer measured the gaseous and dissolved fission products in the loop coolant. A second mobile spectrometer scanned different pipe locations for the depositing fission products. Each spectrum was collected over a 1000-second counting interval during steady reactor operation, and over a 200-second period for

transient conditions. The calculation of the fission-product release rate from the coolant activity concentration in the loop is detailed in Reference 6.

B.2 Fission-Product Release from Defected Fuel

B.2.1 Steady-State Release

The dependence of the release-to-birth rate ratio (R/B) on the decay constant (λ) for both the iodine and noble gas species has been obtained for the defect experiments listed in Table 1, and is plotted in Figure 3. These experiments cover a wide range of defect sizes. A simple linear relationship of the form

$$R/B \propto 1/\lambda^b \qquad [1]$$

holds for each of the following groups of isotopes:

Group I: radioiodines (I-131, I-132, I-133, I-134, and I-135)

Group II: noble gases with short-lived precursors (Kr-85m, Kr-87, Kr-88 and Xe-138)

Group III: noble gases with long-lived precursors (Xe-133, Xe-133m and Xe-135)

The slopes of the lines drawn in Figure 3 are summarized in Table 4, and represent the exponential (b) or release dependency of (R/B) values on the decay constant as given in Equation [1].

In our experimental observations "b" values range from 0.5 to 1.5. Early theoretical considerations by Booth (7) predicted a (b) value of 0.5 for purely diffusive release from the bulk UO_2. This dependence has been confirmed in recent sweep-gas experiments with intact fuel at CRNL at high linear powers (40 to 62 kW/m) (8) and by Halden at a low linear power (23 kW/m) (9). A similar dependence is also found for experiment FFO-103, where the fuel element was machined with many slits along its sheath to minimize the holdup of fission products in the fuel-to-sheath gap. Therefore, any delay in release from elements with defects of a smaller size can be attributed to additional trapping of the fission products in the fuel-to-sheath gap. Based on these experimental observations, a steady-state release model was developed at CRNL.

B.2.1.1 Model Description for Steady-State Release

Fission products generated within the UO_2 matrix are partially released into the fuel-to-sheath gap of the fuel element. With defected fuel, these products migrate in the gap toward the defect site, and eventually are released into the primary coolant. In developing our model, the release mechanisms from the UO_2 and from the gap were considered separately. The major considerations were:

(1) release of fission products from the UO_2 in an operating element occurs principally by diffusion with a small contribution by the surface-fission processes of recoil and knockout;

(2) transport in the fuel-to-sheath gap can be explained in terms of either first-order kinetics or diffusion.

Derivations of the mathematical expressions used in this section of the report have been detailed elsewhere (10,11).

Release from UO_2 Pellets

Above about 1000°C, the fission products migrate primarily by thermally-induced diffusion in the bulk UO_2. For this process, the release-to-birth rate ratio (R/B) displays a $\lambda^{-1/2}$ dependence, as can be described by

$$R_{diff}/B = 3 \left(\frac{D'}{\lambda}\right)^{1/2} H' \qquad [2]$$

where: D' = empirical diffusion coefficient in the UO_2 fuel (s^{-1})
λ = radioactive decay constant (s^{-1})
H' = factor to account for the effect of precursors on the diffusional release of fission products in the fuel matrix (see Table 5)

Below 1000°C, the fission-product release is generally independent of λ and temperature but is activated by the fission event. The fission gas can be released by athermal diffusion in accordance with Equation [2] and at the external surface of the pellet. Release to the steam-filled gap, between the pellets and sheath of a defected element, can occur by direct recoil when a fission fragment is produced within a surface layer equal to its range in the solid UO_2.

$$R_{recoil}/B = \frac{1}{4} \eta' \left(\frac{S_g}{V}\right) \mu_f \qquad [3]$$

where:

η' = the efficiency of particles to stop in the gap (the fragments have sufficient kinetic energy (~80 MeV) to embed themselves in the fuel sheathing)
$\eta' = 2\ t_g/\mu_g$ for $t_g \ll \mu_g$

t_g = thickness of the radial fuel-to-sheath gap

μ_g = maximum range of fission fragments in the gap (microns) [$=23.6/\rho_g$ for a steam filled gap of density ρ_g (g/cm^3)]

μ_f = average range of fission fragments in the UO_2 ($\approx$10 microns)

S_g/V = ratio of the geometric surface area to volume of the UO_2

In Equation [3], the cumulative birth rate is used to account for the decay of the precursor products which are emitted into the gap.

Another temperature-independent process of release is knockout, when either a primary fragment, or energetic particle created in a collision cascade, interacts elastically with a fission-product atom. The release fraction for this low-energy process is:

$$R_{knockout}/B = \left(\frac{S_t}{V}\right) \mu^{ko} I(H) \qquad [4]$$

where: μ^{ko} = range of higher-order knock-on in UO_2 (≈ 50 Å)
S_t/V = ratio of total surface area to volume of the UO_2
$I(H)$ = knockout integral (see Reference (11))

In contrast to the recoil process, the initial kinetic energy of the knock-on is sufficiently low (~200 eV) that these particles can be easily stopped within small cracks in the fuel as well as within the fuel-to-sheath gap.

Transport in the Gap

In the kinetic model, release of fission products from the gap into the coolant is assumed to occur by a first-order rate process. Here, the observed release into the coolant is proportional to the available inventory in the gap.

For this process of release, the observed (R/B) ratio in the coolant is given by the equation

$$(R/B)_{coolant} = \left[\frac{\nu_i}{\nu_i + \lambda}\right] (R_T/B)_{fuel} \qquad [5]$$

where: ν_i = escape rate constant in the gap (s^{-1})
i = iodine (I) or noble gas (N) species
R_T = total release from fuel matrix = $R_{diffusion} + R_{recoil} + R_{knockout}$ (Equations [2, 3 and 4])

Alternatively, transport of the fission products in the steam-filled gap can be considered to be a diffusion phenomenon. Thus, the rate of release from the gap into the primary coolant can be evaluated from the Fick's law of diffusion. For an element of length (ℓ) with (n) defect sites (i.e., sheath perforations) located symmetrically along the sheath, the (R/B) behaviour is given by

$$(R/B)_{coolant} = \left[\frac{2nL}{\ell} \tanh\left(\frac{\ell}{2nL}\right)\right] (R_T/B)_{fuel} \qquad [6]$$

where: L = the "diffusion length", = to $(D_i/\lambda)^{1/2}$,

D_i = diffusion coefficient of fission products in the gap (m^2/s)

In Equations [5] and [6], those terms enclosed in square brackets describe the holdup in the gap of fission products during their transport toward the defect opening.

B.2.1.2 Comparison with Experiment

If diffusion is the dominant release mechanism from the fuel, the gap kinetic model (Equation [5]) yields a release dependence on the decay constant of $\lambda^{-0.5}$ to $\lambda^{-1.5}$, while the gap diffusion model (Equation [6]) yields a behaviour of $\lambda^{-0.5}$ to $\lambda^{-1.0}$. These dependencies are in excellent agreement with the observed results shown in Table 4. In Figure 4, the releases predicted for the recoil and knockout mechanisms for a low-power rating of 23 kW/m were considerably less than the measured releases of noble gas in experiment FFO-102-3 after correcting for the transport of short-lived fission products in the gap. A discussion of the physical significance of fitting parameters in the model has been given in Reference (10).

Fuel oxidation has a significant effect on the diffusion rates of fission gas in the UO_2 matrix. Using the previous gap-transport models, empirical diffusivities (D') can be calculated from measured releases for defected fuel elements, and compared to sweep-gas values where the fuel is essentially stoichiometric (i.e., unoxidized) UO_2 (12). As shown in Figure 5, the effective diffusivities of fission gases are enhanced by several orders of magnitude with fuel oxidation. This is due both to an enhanced gas mobility in the hyper-stoichiometric UO_2 (13), and to a reduction in the UO_2 thermal conductivity causing a bulk temperature increase in the fuel. The diffusion coefficient in experiment FFO-103 is greater than that in the higher-powered test FFO-102-2 because of an increase in oxygen-to-uranium ratio. In test FFO-103 the higher oxide phase U_3O_8 was observed in cracks near the periphery of the fuel pellets, in accord with equilibrium thermodynamics for the oxidation of UO_2 in high-pressure steam (14). However, the limited amount of the U_3O_8 phase implies that the kinetics of this reaction are relatively slow.

B.2.2 Iodine Release Following Reactor Shutdown

B.2.2.1 Model Description

Figure 3 shows that only a small fraction of the fission-product iodine in a defected element is released into the coolant while the reactor is operating at constant power. Most of the iodine available for release is likely present as a liquid-water soluble deposit (such as cesium iodide) on the UO_2 surface or on the inner surface of the Zircaloy sheath. If the temperature in the pellet-to-sheath gap drops below that of coolant saturation, as happens during a reactor shutdown, the water which has entered the element remains in the liquid phase and leaches these deposits. The dissolved iodine then migrates by diffusion along the water-filled gap to the defect site, resulting in an

increased release to the primary coolant during the shutdown period, according to the following expression (15).

$$N_c(t) = \left\{N_{co} + \sum_{j=1,3\ \text{etc}} N_{jo} \left(\frac{\nu}{j^2\ \nu-LR}\right) \left[1 - \exp\left(-(j^2\nu-LR)t\right)\right]\right\} \times \exp\left(-(\lambda + LR)t\right) \quad [7]$$

where: $N_c(t)$ = inventory of iodine in the coolant at time t

N_{co} = initial inventory of iodine in the coolant at the time of shutdown

N_{go} = initial inventory of iodine in the gap available for release at the time of shutdown = $\sum N_{jo}/j^2$ where j=1,3..

ν = escape-rate coefficient = $\pi^2 n^2 D/\ell^2$ where D is the effective diffusion coefficient for iodine in the gap on shutdown and n is the number of defect sites

R = loss-rate constant for coolant leakage and ion-exchange purification in the primary coolant system

Since the higher-order terms in the series expansion (j>1) die out rapidly, the release behaviour can be approximated by the first-order expansion.

Moreover, this expression is also identical to that derived by assuming a first-order kinetic release from the gap.

Based on this model, the time at which the iodine inventory in the coolant reaches a maximum is given by

$$t_{max} = \left(\frac{1}{LR-\nu}\right) \ln \left\{\left[\frac{N_{co}}{N_{go}} \left(\frac{\nu-LR}{\nu}\right) + 1\right] \left[\frac{\lambda+LR}{\lambda+\nu}\right]\right\} \quad [8]$$

B.2.2.2 Comparison with Experimental Data

The CRNL defect test (FFO-109) was designed to investigate the performance of defected CANDU fuel during transient conditions. The defected fuel element was typical of failures discharged from the power reactor, i.e., the element initially contained a manufacturing flaw which had led to the development of localized hydriding and cracked hydrid blisters on the Zircaloy sheath.

A non-linear least-squares fit of the iodine release model using only the first term in the series expansion in Equation [7] to the experimental data for the isotopes I-131 and I-133 is shown in Figure 6. The excellent fit of the theoretical expression to experimental data suggests that the diffusion model may be used to describe the release process. This fitting indicates that approximately 1.4% of the I-131 generated in the fuel during the previous low-power irradiation is available for release after the shutdown.

B.3 Fission-Product Release from Uranium Contamination

Traces of uranium compounds may be found on the surfaces of the primary heat-transport system of power stations. This contamination is caused by uranium loss from defected elements and from the small amount of uranium deposited on fuel-element external surfaces during fabrication. Most of this contamination is in the form of very fine particles. Experiments at CRNL have shown that defected elements release uranium when individual grains of UO_2 are loosened by oxidation along their boundaries.

For small particles of fuel at low temperature, fission-product release may occur by direct recoil and knockout. However, since the range of the fission fragment is about the same size as the UO_2 fuel particle itself, each fragment will leave the individual particle of the fissioning uranium atom and knockout does not occur. Knockout is also negligible, compared to that of recoil, for fuel with dimensions much greater than the recoil range (see Figure 4). For example, experimentally measured ratios of release rates of Kr-88 to Xe-138 were between 0.4 and 0.7 in a pressurized-water loop containing fuel debris on piping surfaces (16). These ratios agree with the theory of recoil. Here the release expression for a small particle of fuel of diameter (d) deposited onto a solid surface, is

$$R/B = \frac{1}{2}\left\{\frac{1}{\alpha^3} + \frac{3\mu_f}{2d}\left(1 - \frac{1}{\alpha^2}\right)\right\} \qquad [9]$$

where $\alpha = 1$ or d/μ_f, whichever is greater. Since B is proportional to the fission yield Y (i.e., $B = \dot{F}Y$ where $\dot{F}$ is the fission rate), and the right side of the above equation is a constant, the calculated release ratio of $R_{Kr-88}/R_{Xe-138} = Y_{Kr-88}/Y_{Xe-138} = 0.55$. In this calculation, the cumulative yield for U-235 has been used to account for the decay of the precursor products emitted into the recirculating coolant.

B.4 Power Station Applications

B.4.1 Steady-State Analysis

When monitoring for fuel failures in the power stations it is important to distinguish the activity release originating from uranium contamination on the in-core surfaces (tramp uranium) from the activity released by fuel failures. This can be achieved as the two sources have distinctly different release processes (see Sections B.2 and B.3).

With defected fuel, the fission products migrate through the UO_2 matrix and then along the fuel-to-sheath gap to the defect site. For fuel ratings greater than about 20 kW/m (see Section B.2.1.2), diffusion is the primary mode of release from the UO_2 fuel (with fuel-element failures diffusion is enhanced because of fuel oxidation by steam). Therefore, using Equations [2], [5] and [6], the release rate when normalized by the fission yield (Y) can be described generally by:

$$R/Y = a\lambda^b H' \qquad [10]$$

where: H' = a dimensionless factor accounting for precursor effects (see Table 5)

Except for I-132 (where H' ≃ 12 because of the relatively long half-life of its tellurium precursor), the H factor is close to unity and can be ignored. The constants (a) and (b) are dependent on the chemical nature of the species. The constant (b) (for both iodines and the noble gases) is strongly influenced by the size, number and distribution of defects in the sheath. When there is little holdup of fission products in the gap, as with many defects located along the length of an element, b = -0.5 corresponding to a high "UO_2 exposure" (Table 6). For defects of smaller size, diffusion of fission products in the gap becomes important, and b = -1.0. However, with small failures there is an additional chemical holdup of radioiodines in the gap, controlled by iodine dissolution from the fuel and sheath surfaces, where b = -1.5. For uranium contamination, Equation [9] shows that the R/Y is independent of λ such that R/Y is a constant (=1/2 F), assuming that the range of the fission fragment is comparable to the diameter of the fuel particle itself. (F is the fission rate in fissions/second.) The different sources of release in the power reactor can then be mathematically separated by the expression:

$$R/Y = a\lambda^b + c \qquad [11]$$

B.4.1.1 CANDU Reactor System

A typical example of using Equation [11] (in analyzing fission-product release data for the Point Lepreau CANDU reactor) is illustrated by Figure 7. Here, the release rate is calculated from the steady-state activity concentration in the coolant for the various isotopes of iodine. This release is normalized by the fission yield, Y, and then plotted against the decay constant. The fission yield has been corrected to include fissioning of the Pu-239 formed by U-238 capture.

The release curve in Figure 7 indicates the presence of both defected fuel and uranium contamination in the reactor. There is a superposition of the two release processes, e.g., the release curve is sloped for the longer-lived isotopes, but is independent of decay constant at $\lambda > 2 \times 10^{-5}$ s^{-1}. For the defected fuel contribution, a value of b = -1.3 points to a small defect with the amount of UO_2 exposure in the coolant between 1 and 11 mm^2 (see Table 6). Since the release of I-131 is due mainly to fuel failures, its release rate can be used to estimate the number of in-core failures. Normalizing the measured I-131 release by a single element value of 6×10^{11} atoms/s*, a single failure is predicted. This prediction is consistent with on-line

* This value is based on previous experience with defected fuel in the Douglas Point and Pickering reactors, where the number of fuel-element failures was known (17).

gaseous fission product (GFP) monitoring. A step increase in the Xe-133 coolant activity levels was observed prior to the sampling period shown in Figure 7. These levels began to decrease at a natural rate of decay after the suspected fuel channel was refuelled. A single failure was later confirmed by wet sipping techniques and visual inspection in the reactor underwater bays.

Finally, the amount of fuel debris (m_U (kg)) in the core can be estimated from the fitted parameter $C \simeq \frac{1}{2} \dot{F}$ (~1.3×10^{12} fissions/s) based on an average neutron flux (ϕ) of 8.0×10^{13} n/cm^2.s, such that (11)

$$m_U = \frac{C}{0.20\ \phi\ Z \underset{\substack{i=U\text{-}235 \\ P\text{-}239}}{} (w\ G_F\ g_f/A)_i} \qquad [12]$$

where: w = weight fraction of fissile material (gm/kg natural uranium)

G_F = microscopic fission cross section (barns) 580 for U-235, 742 for Pu-239

g_F = non 1/v fission factor, 0.94 for U-235, 1.33 for Pu-239

A = atomic mass of fissionable isotope (g/mole)

Using equation [12], approximately 4 grams of uranium are estimated to be deposited on the in-core surfaces. This value agrees with that determined by DN monitoring techniques (18).

B.4.2 Iodine Transients in CANDU Reactors

The size of the "iodine spike" on reactor shutdown can also provide information on the number of fuel failures. In our experimental loop the peak in iodine concentration in the coolant (t_{max}) occurs after about a day for the isotope I-131 (see Figure 6). However, in power stations, this peak occurs earlier because of the continual operation of the coolant cleanup system. For instance, with a purification constant of LR = 6×10^{-5} s^{-1}, a peak is predicted in just six hours using Equation [8]. Normalizing the observed value of 28 300 GBq in the Pickering Unit 3 reactor to the single element value ($N_C(t_{max}) \simeq 1440$ GBq*), a defect rate of 0.016% is predicted. This value agrees with the value of 0.022% calculated from steady-state I-131 activity measurements (i.e., see Section B.4.1.1). This period of unusually high coolant activity during 1973 was a result of power-ramp defects prior to the introduction of a graphite interlayer (CANLUB) on the inner surface of the Zircaloy cladding, and better fuel management.

* In this calculation, it is assumed that $N_{co} \ll N_{go}$ where $N_{go} \sim 5920$ GBq of I-131 for a power-ramp failure; this number is based on Pickering experience, where the number of failures was known from post-irradiation examination.

C. ONTARIO HYDRO CANDU STATION EXPERIENCE IN DETECTING AND LOCATING DEFECTED FUEL (M.R. Floyd and P.T. Truant)

Ontario Hydro presently operates 4 commercial multi-unit CANDU nuclear generating stations, each consisting of 4 CANDU-PHWR-type reactors (Table A). Two of these multi-unit stations are located at the Pickering site (PNGS-A and PNGS-B), while the remaining two are at the Bruce site (BNGS-A and BNGS-B). A fifth multi-unit station is under construction at the Darlington site (DNGS). The monitoring systems used to detect and locate failed fuel in Ontario Hydro stations are also described in Table A.

C.1 Detection of Failed Fuel Using Gaseous Fission-Product Monitors

The presence of defected fuel in Ontario Hydro reactors is detected by monitoring fission-product concentrations in the coolant using gamma-ray spectrometry. Isotopes monitored are the gaseous and dissolved fission products (i.e., noble gases and radioiodines).

In addition to on-line monitoring for I-131 because of its biological hazard, coolant activity data may also be analyzed to estimate:

(1) The amount of tramp uranium in the core and its associated fission-product release.

(2) The release of fission products from defected fuel during periods of steady reactor power.

(3) The predominant type of defected fuel in the core (small defects at low power versus large defects at high power).

(4) The equivalent number of defected fuel elements in the reactor core.

C.1.1 Estimating the Release of Fission Products from Tramp Uranium Versus Defected Fuel in Ontario Hydro CANDU Reactors

The ability to distinguish between releases from tramp uranium and defected fuel is essential in assessing the in-reactor performance of the fuel. For example, an increase in release of fission products from both tramp and defected fuel elements may indicate the onset of large defects releasing fuel to the coolant. Similarly, a steady tramp release accompanied by an increase in release of soluble and gaseous fission products from defected fuel would point to a growth in the number of small defects.

The fission-product release from tramp is distinguished from that of defected fuel by fitting yield-corrected release rates for fission gases and radioiodines to a curve of the form shown by Equation [11].

Figure 8 shows a typical plot of (R/Y) versus (λ) data for radioiodines from Bruce B, Unit 6. The ($a\lambda^b$) term in Equation [11] represents the yield-corrected release from defected fuel, while the (c) term represents the release from tramp uranium. Experience with Ontario Hydro reactors has shown

that the yield-corrected release from I-134 is an excellent approximation for fission products released by the tramp uranium in core.

If the actual value of (R/Y) for an isotope calculated from coolant concentration data is $(R/Y)_{TOT}$, then the value of R/Y from defected fuel, $(R/Y)_{DEF}$, in the core is:

$$(R/Y)_{DEF} = (R/Y)_{TOT} - c = a\lambda^b \quad [13]$$

In terms of release rates, this becomes

$$R_{DEF} = R_{TOT} - cY \quad [14]$$

where: R_{DEF} = isotopic release rate (atoms/s) from defected fuel

R_{TOT} = isotopic release rate (atoms/s) from both defected fuel and tramp uranium calculated from coolant concentration data

c = tramp uranium contribution to R/Y (constant for all isotopes)

If there is a negligible tramp uranium in the core, then $R_{TOT} = R_{DEF}$.

C.1.2 Estimating the Predominant Type of Defected Fuel in the Core

The presence of defected fuel in a CANDU core may present a dilemma for the reactor operator in absence of detailed knowledge about the extent and number of the failure(s). The premature discharge of fuel from a channel suspected of containing failures results in an economic penalty due to lost burnup, and the core physics may be perturbed by a premature refuelling. However, defected fuel left in a reactor may deteriorate and release large quantities of radioactive fission products, thereby increasing the man-rem dose to reactor operators and, in extreme cases, exceeding licensing limits (19). Hence, reactor operators need to characterize the type of failures and use the information to establish a priority for the removal of defected fuel.

Research at CRNL and experience at Ontario Hydro have shown that a power threshold of 40 kW/m exists above which extensive secondary deterioration to a fuel element is caused by sheath hydriding (20). (These elements are commonly referred to as "unstable failures".) It is therefore prudent to discharge defected fuel operating above this power level as soon as possible. Conversely, at powers <40 kW/m, the possibility of secondary damage to the element is very small, as is both the fission product and tramp uranium release to the coolant (called "stable failures"). (Fuel elements with tiny defects that release quantities of fission products insufficient to be detected by the reactor monitoring systems are of little concern to operators until secondary damage occurs.)

These two widely differing "types" of defected fuel may be distinguished from one another by using the measured ratios of fission-product release rates from specific isotopes. The preferred ratios used by Ontario Hydro for this application are Xe-133/I-133 and Xe-133/I-131 (Figure 9). These ratios show a strong correlation with defected fuel type and have little or no burnup dependence.

Fission-product ratios for Bruce B, Unit 6, are plotted on Figure 9 and both fall in the top end of the stable defect region, suggesting that the defect at this particular time was not deteriorating rapidly and releasing uranium. Post-irradiation examinations of discharged fuel revealed an element irradiated at 35 kW/m with a defect hole of 1.5 mm^2.

C.1.3 Estimating the Equivalent Number of Defected Fuel Elements in the Core

Once the predominant type of defected fuel in the core has been determined, the equivalent number of defected elements can be estimated as follows:

$$\text{Number of defected elements} = \frac{\text{observed release rate from defected fuel in the reactor primary cooling system}}{\text{known release rate for a single defected fuel element (see Figure 9)}}$$

The preferred isotope used by Ontario Hydro for this calculation is Xe-133. The Xe-133 release rate per defected element, as determined from experimental single-element irradiations (Section B), is shown as a function of sheath deterioration in Figure 9.

For the Bruce B Unit 6 situation used as an example of defect type, the number of defects in-core translates into 1 to 3 elements.

C.2 Locating Defected Fuel in Ontario Hydro CANDU Reactors

Once the presence of defected fuel has been detected in a CANDU core, reactor operators locate the failure(s) so that fuel bundles can be removed from the correct channel. As indicated earlier, two failed-fuel location systems exist in Ontario Hydro CANDU stations:

(1) DN Detection System (Bruce NGS-A and B).

(2) Feeder Scanning System (Pickering NGS-A, B and Darlington NGS).

C.2.1 Locating Defected Fuel by DN Monitoring

The DN System operates by detecting "delayed" neutrons emitted from the predominant DN precursors, Br-87, and I-137, with half-lives of 56 and 23 seconds, respectively. A sample line runs from the outlet of each fuel channel to a DN monitoring room, where the DN signal from each channel is monitored individually in the absence of "prompt" neutrons. Since the DN precursors are short-lived, DN monitoring is done with the reactor at power.

All fuel channels normally give rise to some DNs. This "background" signal is from tramp uranium throughout the core. Channels containing defected fuel will exhibit a signal above that of the normal background, so "suspect" channels are identified on the basis of their signal-to-background or Discrimination Ratio (DR). Historically, a DR $\geq$ 1.3 indicates the presence of defected fuel in that particular channel, as illustrated in Figure 10, which shows the DN signals from a row of 30 channels in the Bruce B Unit 6 reactor. One channel, M07, with a DR of about 1.8, contains defected fuel. As a follow-up to the DN scan, channel M07 was discharged and the bundles inspected in the underwater bays. A defected outer element was observed in the bundle discharged from channel position No. 9. The failed element had operated at a linear power of 35 kW/m and the defect size was about 1.5 mm^2 (see Section C.1.2).

C.2.2 Locating Defected Fuel by Feeder Scan Monitoring

The feeder scanning system operates on the principle of detecting gamma-rays emitted from fission products that deposit rapidly on the outlet feeders of channels containing defected fuel. The half-lives of the deposited fission products range from 6 hours (Tc-99m) to 368 days (Ru-106/Rh-106) with the most predominant isotopes being Zr-95, Nb-95 and La-140 (19). The gamma signal from each channel is monitored by passing a Geiger-Mueller detector amongst the outlet feeders via guide tubes. Scans have been performed successfully only during shutdowns in the absence of large, high-energy gamma fields emanating from short-lived D_2O activation products.

During a shutdown, all outlet feeders have a background gamma field, caused mostly by activated corrosion products. In addition to this "background" signal, outlet feeders of channels containing defected fuel emit gamma-rays originating from fission products deposited on the surfaces of the piping. The concentrations of the depositing fission products are the highest in the coolant and on the outlet feeder of a channel containing defected fuel. Figure 11 shows the gamma signal from a row of outlet feeders in Pickering Unit 6, one of which (channel F12) contains defected fuel.

D. CANADIAN CANDU-6 STATION EXPERIENCE IN DETECTING AND LOCATING DEFECTED FUEL (A.M. Manzer)

Two CANDU 6 reactors are currently in service in Canada: one station, Point Lepreau, is owned and operated by the New Brunswick Power Commission, and the second, Gentilly-2, is owned and operated by Hydro Quebec; see Table A. Both units have the same basic design, layout of major components and operating systems. Two failed-fuel detection systems, the GFP monitor and DN system, which operate independently of each other, are described in Table A (21).

D.1 Detection of Defected Fuel Using GFP Monitors

The GFP monitors in the CANDU 6 stations are computer-controlled, high-resolution gamma-ray spectrometers. They are designed to operate continuously, repeatedly measuring the gamma-ray activity of the gaseous fission products, Xe-133, Kr-88 and Xe-135, and of iodine-131 in sample flows from

each of the two heat-transport system loops. Two sample lines, one from each loop, carry the coolant from the pump discharge to the sample holders. The sample transit time is about 15 minutes, which ensures sufficient time to remove unwanted F-17 by radioactive decay. Either loop 1, loop 2 or both loops together (without mixing), can be monitored. This enables the operator to determine which loop contains a defected fuel bundle.

The three GFPs and the radioiodine monitored by the GFP system were chosen for the following reasons. Xe-133 is a long-lived fission product which has a high release rate from defected fuel. Its concentration, when compared to that of the short-lived fission gas, Kr-88, provides information on the source, the extent of sheath damage (deterioration) and the buildup of tramp uranium in the core. Xe-135 provides data on iodine release rates when high purification flows to the ion-exchange columns are removing the radioiodines from the coolant. Since the noble gases are not retained by the ion-exchange resins, the I-135 in the ion-exchange system becomes a secondary source of Xe-135. I-131 is monitored because of its biological hazard. Since its concentration in the coolant is suppressed by the ion-exchange system, it is not a reliable indicator for assessing fuel damage.

D.1.1 Interpretation of GFP Data

In the CANDU 6 reactors the specific radioactivities of Xe-133 and Kr-88, measured in MBq per kilogram of coolant, are analyzed to determine the source of fission-product release in the core. Three sources are defined:

1) A fast-release defect - the release mechanism is primarily controlled by the diffusion process of the gases through the fuel matrix with very little holdup inside the fuel element (an "unstable" defect).

2) A slow-release defect - the release of the fission gases is restricted by a small-sized defect. A large fraction of the short-lived fission products is lost by decay during the delay in the fuel-sheath gap between birth by fission and release from the element to the coolant (a "stable" defect).

3) Tramp uranium - the fission gases are released promptly at birth by the recoil process. There is very little, if any, gas retention within the small amounts of tramp uranium distributed on the heat-transport system surfaces within the core.

Table D.1 summarizes the release characteristics for the three sources during steady-state and transient conditions. The following sections give the basis for these numerical values and their application to CANDU 6 conditions.

TABLE D.1

FISSION-GAS RELEASE CHARACTERISTICS FOR THREE SOURCE TYPES

	SLOW RELEASE DEFECT (Stable)	FAST RELEASE DEFECT (Unstable)	TRAMP URANIUM
Steady-State Conditions			
Xe-133 Fractional Release (F)	0.05 - 0.10	0.10 - 0.20	1.00
Corresponding Xe-133 Release Rate ($\overline{R}$) in atoms/s	2×10^{12} to 4×10^{12} at 40 kW/m	4×10^{12} to 8×10^{12} at 40 kW/m	5×10^{10} per gram U
Fractional Release Dependence* on Natural Decay (λ)	b = 1.0	b = 0.5	b = 0.0
Transient Conditions			
Burst Release Fraction for Xe-133	0.05	0.05	0.0

* $F \propto 1/\lambda^b$

D.1.2 Estimating the Number of Defected Elements and Tramp Uranium Levels from Steady-State Release GFP Data

The mass balance equations governing the fission-product inventories within the fuel elements and heat transport system can be used to derive an expression for the number of defected fuel elements (n_{def}) in the reactor core. During steady-state conditions, when the activity concentrations are at equilibrium and the reactor power, coolant pressure and temperature are constant, the relationship becomes:

$$n_{def} = \frac{\lambda^* Q}{R} \qquad [15]$$

where: λ^* = the system decay constant (s-1) is the sum of all losses due to natural radioactive decay (λ), to removal by the purification systems (β) and the coolant leakage (γ'). For the noble gases Xe-133 and Kr-88, the radioactive decay term dominates and the other losses can be neglected.

Q = the number of isotope atoms in the coolant determined directly from the measured coolant activity

R = the release rate (atoms/s), from one defected element estimated from experimental irradiations or from operational experience

The release rate (R) can be determined from the expression

$$R = (F)\ \dot{FY} \qquad [16]$$

where: $\dot{FY}$ = the source term which is the product of the decay chain yield (Y), in (atoms/fission) and the fission rate for the fuel element ($\dot{F}$), in fissions/second, which is power dependent. (F) = the fractional release, or release-to-birth rate ratio, i.e., R/B.

In experimental irradiations at CRNL, the fractional release for Xe-133 varied from 2 to 5% for a drilled hole defect in a fuel element operating at a linear power of 48 kW/m. In another CRNL test at powers of 55 kW/m, the release varied from about 5 to 17% for fuel elements having either drilled holes or a machined slit (22). Using this information, the fractional release for Xe-133 in CANDU 6's was arbitrarily set at 5 to 10% for a slow-release defect, at 10 to 20% for a fast-release defect, and at 100% for tramp uranium in the core. Using these (F) values, one defected element in the reactor core, operating at 40 kW/m, will account for Xe-133 activity concentrations of 17 to 34 MBq/kg for a slow-release defect, and 34 to 68 MBq/kg for a fast-release defect. Tramp uranium distributed uniformly in the core and irradiated at the average neutron flux level, will yield 0.8 MBq/kg for one gram of uranium. These predictions are based on a heat-transport system inventory of 122 Mg heavy water and an energy yield of 200 MeV/fission.

D.1.3 Estimating Number of Defected Elements from Transient Releases

Fission gases can escape in short-lived bursts from defected elements under various transient conditions, such as a sudden change in coolant pressure, temperature or power. For example, a power increase may cause the water inside the element to flash, expelling steam and fission products to the coolant. On the other hand, a power reduction may cause thermal cracking of the UO_2 pellet, thereby releasing the gases from the matrix to the gap and eventually to the coolant. Furthermore, a transient release of the noble gases also occurs when the fuel element initially fails and releases a portion of its "free" inventory of noble gases. In all transient release situations, the portions of the total noble gas inventories escaping from a high-powered defected fuel element (~40 kW/m) is in the order of a few percent: about 5% for Xe-133, 0.5% for Kr-88, and 0.2% for Xe-135 (23).

Based on these burst-release fractions, it is possible to estimate the equivalent number of high-powered defected elements in the core from the increases in coolant activity concentrations. The Xe-133 activity concentration will increase during a transient by about 20 MBq/kg per defected element operating at 40 kW/m.

D.1.4 Assessing the Defect Type from the Measured Concentration Ratios of Specific GFPs

The dependence of fractional release (F) on the inverse of (λ^b) is a well-established technique for assessing the source of the coolant activity (24,25). For tramp uranium within the core, all fission gases are released promptly at birth, causing (F) to be independent of the decay constant with the exponent (b) equal to zero. For defected fuel elements, the fission-gas release is primarily governed by the diffusion process in the fuel matrix for fast-release (unstable) defects, or by the hole size in the element sheath for slow-release (stable) defects. In both cases, there is a delay between birth by fission in the fuel and the release through the hole into the coolant. The portion of inventory available for release to the coolant depends on this time delay and on the decay half-life of the GFP. Therefore, the fraction of the inventory released from the fuel is higher for the longer-lived gases and the exponent b is positive. For data interpretation purposes, a value of 0.5 is assigned to b for a fast-release defect and 1.0 for a slow-release defect.

These relationships can be used for comparing the concentrations of long-lived Xe-133 (5.3 day half-life) with short-lived Kr-88 (2.8 hour half-life).

Assuming negligible losses at equilibrium other than those due to natural decay, the activity concentration ratio for Xe-133 to Kr-88 can be expressed in terms of the chain yields, decay constants and exponent b:

$$\frac{[\text{Xe-133}]}{[\text{Kr-88}]} = \frac{Y_{Xe}}{Y_{Kr}} \left(\frac{\lambda_{Kr}}{\lambda_{Xe}} \right)^b \qquad [17]$$

where the ratio = 2 to 3 for tramp uranium
= 12 to 20 for a fast-release defect
= 80 to 130 for a slow-release defect

The upper end of each range reflects the adjustment on the chain yields due to the plutonium buildup at high burnup.

The Xe-133 to Kr-88 activity concentration ratio can be a useful technique for assessing the defect type, but only for certain operating conditions. Firstly, the activity concentrations must be at equilibrium. Equilibrium is approached when the fission gas within the fuel defect builds up to its equilibrium inventory at steady power. This is normally achieved when the fuel defect operates at steady power without further degradation for about three decay half-lives of Xe-133, or about two to three weeks of steady power operation. Secondly, the presence of tramp uranium in the core provides a source of fission gas that desensitizes the ratio technique, as shown in Figure 12. Defect types can be distinguished only when the loop contains small amounts of tramp uranium, about 3 grams within the core boundaries. Consequently, the ratio technique is only used under the specific conditions given above.

D.2 Location of Defected Fuel Using DN Monitoring

The DN monitoring system has two basic functions in a CANDU 6: the first is to locate the fuel channel containing the defected fuel, and the second is to locate the position of the defect within the fuel column (23). The data can also be analyzed to determine when defected fuel deteriorates and releases large amounts of uranium to the coolant.

Sampling lines from each of the 380 fuel channels in the reactor carry coolant to the sample coil arrays in two water-filled moderator tanks, one in each scanning room. Six BF_3-filled neutron detectors in each room are positioned by their carriage and lowered into the sample-coil dry wells. The data are collected during the preset counting time and analyzed by an on-line computer. The detectors are raised and repositioned in sequence until all channels have been scanned. Computer-controlled or manual operation is done from a separate room in the reactor building. One complete DN scan requires only a few hours and is normally done every one to three weeks. The design of the sampling lines incorporates a deliberate 50-second delay to eliminate interference from the unwanted activation products, the photoneutron producing nitrogen-16 (7-second half-life) and the neutron-emitting nitrogen-17 (4-second half-life). The detectors monitor the neutron-emitting fission products, I-137 (22.3-second half-life) and Br-87 (55-second half-life). Background gamma radiation is rejected by electronic discrimination.

The parameters measured by the DN system are: (A) and (B), the average DN signal count rates of the channels in each of the two loop-halves (designated as loop-half A and B), and (S), the DN signal count rate for a single channel.

In practice, (S) is normalized to the loop-half average and is expressed as the discrimination ratio (DR) for a fuel channel:

$$DR = S/A, \text{ or } S/B \qquad [18]$$

D.2.1 DN Data Interpretation

The DN data analysis is based primarily on two calculated parameters:

- the DR for each channel, and
- the loop average DN signal count rate normalized to full power.

The DR is equal to the DN signal of a fuel channel divided by the average signal. A fuel channel in a CANDU 6 is suspected of containing a defected element if its discrimination ratio is significantly higher (about 30%) than the average for neighbouring channels, or is increasing with time (26). The

minimum number of defected elements in the core at any time is equal to the number of suspect channels. This guideline is generally true because most fuel defects have been single-element failures.

The best parameter for indicating uranium release in the core is the loop-average, DN count rate. This count rate is the average of the signals from about 190 channels in each loop, and is proportional to the concentration of the DN emitting fission products, I-137 and Br-87. These fission products are released primarily from the uranium that is deposited on the primary circuit surfaces within the core boundaries. Only a small portion of these fission products comes from fuel defects. For example, if one defect increases the DN signal of a channel by 30%, then the average signal for the 190 channels in one loop increases by about 30/190 = 0.2%. The average DN signal provides a benchmark for establishing other fission products as uranium release indicators.

Special single-channel DN monitoring is done to locate the position of the defected fuel bundle within a suspect channel during refuelling at power. By watching the changing DN signal as a fuel defect moves through the core, the position of the failed bundle can be estimated.

D.2.2 Assessing the Condition of Defected Fuel

Figure 13 shows the DR and loop-half average signal behaviour for a defected element in loop-half A, deteriorating under one of two hypothetical conditions:

(1) no uranium release, but increasing defect hole size, and
(2) uranium release, but stable hole size.

By predicting the DR behaviour of suspect channels for these two cases, the dominating type of deterioration of defected fuel can be determined from the DN data trends.

The first set of curves on Figure 13 represents the signal behaviour for a fuel defect that is not releasing uranium but has a defect hole size that is increasing. The DR increases because the defect hole size is increasing, allowing fission products to escape at a higher rate. The loop-half average DN signals will also increase, but at a much slower rate due to both the dilution and mixing effects in the loop and the activity decay during recirculation. The starting point for each curve is at DR = 1 at the time of failure. The corresponding starting value for (A) reflects the tramp uranium level in the loop.

The second set of curves on Figure 13 represents a fuel defect that is releasing uranium but has a stable defect hole size. At steady loop conditions, the hole size sets the fission-product release rate, and (S-A) will be constant, as shown by each curve. However, the loop-half average signal will increase as the tramp uranium builds up in the core.

In practice, both types of deterioration are occurring simultaneously in defected fuel. However, by plotting the DN data trends in the manner suggested by Figure 13, it is possible to determine when one type dominates over the other.

It should also be noted that a certain portion of the uranium, released from a defected element, may deposit immediately downstream within the core boundaries of the suspect channel. If this happens, the tramp uranium will act as a secondary source of fission products in that channel and it would not be possible to determine whether the increasing DR is due to a tramp uranium buildup in the channel or due to an increasing defect hole size.

D.3 Experience at Point Lepreau with Defected Fuel

The first CANDU 6 reactor to go critical was Point Lepreau in 1982 July. It was declared in-service in 1983 February, and refuelling started that March. In 1983, four defected fuel bundles were discharged from four fuel channels (26). In 1984, one fuel bundle was visually confirmed as having failed. In the first half of 1985, one more failed fuel bundle was discharged. These six fuel defects are summarized in Table D.2.

TABLE D.2

VISUALLY CONFIRMED FUEL DEFECTS
AT POINT LEPREAU (TO 1985 MARCH)

BUNDLE POSITION (channel and location)	NUMBER OF DEFECTED ELEMENTS AND PREDOMINANT LOCATION OF SECONDARY DAMAGE TO ELEMENT SHEATH	ELEMENT LINEAR POWER (kW/m)	DISCHARGE DATE
Q16 - 2	2-3 - upstream end	8	83.4.19
G11 - 5	1 - upstream end	24	83.4.24
R09 - 3	1 - upstream end	38	83.4.25
R15 - 7	1 - middle	42	83.6.15
L22 - 10	1 - downstream end	17	84.6.22
S12 - 10	1 - upstream end	32	85.2.4

As an example of defect behaviour at Point Lepreau, Channel S12 was refuelled on 1984 December 10, with a normal eight-bundle shift. Several days later, its DR began to increase, coinciding with an increase in the Xe-133 activity (December 31). Since none of the new bundles had sufficient fission-gas inventory to contribute to the Xe-133 transient release, the defect was believed to be in one of the four downstream bundles.

During refuelling on 1985 February 4, the single-channel DN scan indicated that either bundle 9 or 10 had failed. Inspections in the fuel bay confirmed

that bundle 10 contained one defected fuel element. Fuel-management data indicated the defected element had operated at 32 kW/m since the time of failure.

Prior to the S12 fuel failure, the Xe-133 and Kr-88 activity concentrations were at equilibrium: about 2 and 0.6 MBq/kg, respectively. The Xe-133 to Kr-88 ratio was equal to about 3, indicating the main source of activity was due to tramp uranium. Approximately 2 to 3 grams of tramp uranium were believed to be located in the core (Figure 12). Since the corresponding loop average DN signal, at the time, ranged from about 250 to 300 counts per second, the uranium contamination level was estimated at 8 to 10 times that of a new core. Combining both GFP and DN data, the contamination due to fuel fabrication on bundle surfaces was estimated at 6×10^{-9} to 10^{-8} grams of uranium/cm^2. This range is well below the new fuel specification by about a factor of 2 to 3.

D.3.1 Xe-133 Activity Releases Detected by the Point Lepreau GFP System

In Figure 14, the steady-state Xe-133 activity concentrations are plotted against the linear powers of the defected elements. The criteria for identifying defect types (22,27) included in this figure suggests that the fuel defects in channels Q16, G11 and R09 were likely fast-release defects, and the ones in L22 and S12 were slow-release defects.

In Figure 15, the increases in Xe-133 activity due to a transient release are plotted against the linear powers of the defected fuel elements. Most of these transients occurred while refuelling the channel containing a fuel defect. As shown, most of the burst-release fractions were less than 10% of the total Xe-133 inventory within the defected element. The burst-release fraction is more dependent on bundle position than on linear power. This observation supports the fission-product release mechanism associated with water flashing to steam. A defected element near the channel inlet will contain more water, due to the coolant and saturation temperature profile along the channel, than fuel defects further downstream. As the defected bundle is moved downstream during refuelling, the water flashes, expelling steam and fission products into the coolant. The amount of fission products released likely depends on the amount of water inside the fuel element before the move.

D.3.2 Tramp Uranium Release as Detected by DN System

Figure 16 shows the total amount of tramp uranium (c), in the core for each loop, plotted against reactor energy in full power days. The term (c), normalized to 1.0 for a new core, is also proportional to the loop average DN signal, normalized to 100% reactor power. The length of time each confirmed fuel defect resided in the core is also indicated on the figure. The dramatic increase in the tramp uranium level, shortly after the initial startup, was likely due to the fuel defects in channels Q16, G11 and R09. For channels L22 and S12, there was no noticeable change in the average signals, indicating very little, if any, uranium release from these failed bundles.

The average DN signals increased slightly following long shutdowns. This may be due to some chemical/temperature effect on uranium adsorption on heat-transport system surfaces. Also, the marked increase in the average signal for loop 1 during the period from 200 to 300 full power days may have been caused by the release of uranium from another fuel defect that was not located or visually confirmed. During this period, transient releases of Xe-133 activity were also detected by the GFP system.

Figure 17 shows the ratio of in-core uranium contamination ($\dot{a}/\dot{b}$) between loop-halves for loop 1 and 2. The ratio ($\dot{a}/\dot{b}$) is a function of the loop-half average DN signals, described in Reference 18. The ratio increased significantly while the fuel defects were located in loop-half "B" of loop 1 (Q16) and in loop-half "B" of loop 2 (G11 and S12). This increase was due to the uranium release from the defects. Deposition in the core first occurred downstream in loop-half "A" of both loops. After these defects were removed, the ratio decreased towards unity, indicating the uranium distribution was becoming more uniform. This ratio was not affected by the presence of a fuel defect in L22 and S12, providing additional evidence that these defects did not release uranium.

D.3.3 Uranium Release from Defected Fuel Elements

Figure 18 is reproduced from Figure 13, showing uranium release thresholds derived from Point Lepreau experience. The first broad-band curve represents the range of discrimination ratios and loop-half average signals where a single-element fuel failure (R09 and G11) began to release uranium. The second curve represents the threshold for uranium release from a multi-element failure (Q16). The discrimination ratios for channels L22 and S12, before refuelling, fell below the first threshold.

E. Identification and Storage of Failed Fuel Bundles in Fuelling Machines and in Underwater Bays

E.1 Identification of Defected Fuel in the Fuelling Machines and Transfer Link

After the fuel bundles from a suspected defect channel have been discharged into a CANDU 6 fuelling machine, the cooling water in the machine magazine is partially drained into a tank. At Point Lepreau this tank is equipped with radiation monitoring instruments which record the fission-product activity level in the tank water. Any increase above the normal activity measurements signifies the presence of failed fuel in the fuelling-machine magazine. This procedure offers a quick confirmation that defected fuel has been removed from a suspected channel.

Both Ontario Hydro and CANDU 6 reactors have installed radiation measuring instruments to monitor the air (dry sipping) in the transfer mechanisms that link the fuelling machines with the underwater bays (28). Irradiated fuel bundles are discharged from the fuelling machines into the transfer mechanism in pairs. During this transfer each bundle spends a few minutes in air. Air in the transfer tunnel is monitored for gross activity as each bundle pair is

moved; these air samples can detect which pair contains a medium to large defect. All bundles increase the gamma signal of the monitors because of external sheath contamination (especially true if the bundles have been in the same channel with a failed bundle with large amounts of exposed fuel). Defected bundles releasing fission products generate signals above normal background level, as illustrated in Figure 19. At some Ontario Hydro stations, the time the bundle spends in the transfer tunnel can be lengthened to improve the sensitivity of the monitoring systems. Once suspect bundle pairs are identified, they are set aside in the underwater bays for detailed inspection.

E.2 Inspection of Defected Fuel in the Underwater Bays

Because CANDU fuel is inexpensive, the Canadian nuclear utilities make no attempt to repair or reconstruct fuel bundles by replacing defected elements in the reactor underwater bays. Bay inspections are confined mostly to examining suspect bundles to: (a) confirm that a bundle has failed, (b) identify the failed element(s) and (c) determine the failure mechanism. The principal tools for inspecting the fuel underwater is the optical periscope or a radiation-hardened TV camera, along with their associated staging and lighting. These systems have been described in detail in the Phase I report of this Research Project (29). The bays of all Canadian power stations are equipped with identical or similar viewing systems.

Point Lepreau has a system (wet sipping) for identifying defected bundles in the bays, by analyzing water samples taken from the vicinity of suspected fuel bundles. The suspected bundle is placed in a closed can underwater, and the bay water is flushed from the can by clean water supplied through inlet and outlet water lines. The suspected bundle is allowed to sit for some time in the clean water and samples of this water are then collected and analyzed for fission products.

Specialized equipment has been developed at CRNL for identifying defected fuel bundles underwater, and quantifying the release of fission products from the fuel. While still experimental, this apparatus, which is very sensitive to the presence of fission products, is adaptable to the underwater bays of CANDU power stations.

The CRNL apparatus consists of a heavy stainless-steel frame with a fixed horizontal semi-circular tray for holding a fuel bundle. At one end of the tray a vertical end plate is mounted, which contains water, air, electrical and thermocouple lead lines. The tray has two electrical heaters mounted along each side. A stainless-steel can moving on horizontal guide rails can be slid over the tray and mates with the end plate to form a sealed chamber around the tray; see Figure 20. Loading the bundle into the tray, moving the can over the tray, and sealing the can to the end plate are all operations carried out with long-handled tools. Once the can is sealed, the suspect bundle can be surrounded with either warm water or heated air. Both the air or water can be recirculated past a germanium detector of a gamma-ray spectrometer to measure the concentrations of fission products in the flowing system. Thermocouples and pressure sensors are attached to the tray to ensure that

fuel-cladding temperature and can pressures are kept with safe limits during the leak-testing procedure. A lucite hood mounted about a metre above the can ensures that GFPs inadvertently released from the fuel are collected and bled off into the reactor exhaust system. Because the CANDU bundle is short, the apparatus is relatively compact, with an overall surface dimension of just 0.3 m x 1.3 m.

This apparatus has been successfully used to leak test suspected fuel bundles irradiated in the NRU reactor at CRNL. Isotopes of krypton and xenon were detected and measured by the spectrometer system, with air flowing through the chamber. Xenons and radioiodines were identified in a water-filled can. The release of xenon and krypton from the bundle in air was very sensitive to fuel temperature in the can, with activity levels increasing by factors of 4 to 5 when the sheath temperature of the suspected fuel was raised from about 60 to 100°C.

E.3 Storage of Defected Fuel Underwater

With the exception of an interim storage in the inspection bay, defected fuel bundles in both Ontario Hydro and CANDU 6 reactors are generally treated no differently from normally discharged fuel (30). The bundles are stored in open stainless-steel containers called either baskets, trays or modules; see Figure 21. However, failed bundles are usually stored in a special location in the bays. During the early stage of operation at the Ontario Hydro and Point Lepreau power stations, all failed bundles were stored in stainless-steel tubes with a removable end plug. The tubes were loaded underwater and the plug inserted with underwater tools. Since these plugs contained a drilled hole and were not leak tight, the main purpose of these containers was to prevent the release of fuel particles to the bay water. The use of these containers has largely been discontinued and the containers are now used only as a contingency for bundles which are severely deteriorated.

During a period in 1972, when the Pickering nuclear station experienced many fuel defects, failed fuel in the bays released sufficient quantities of iodine to generate high airborne iodine activity. Additions of hydrazine to the bay water reduced the oxidized forms of radioiodine, which significantly reduced the airborne iodine activity. Hydrazine also effectively reduced the release of radioiodines when fresh defected bundles were first discharged into the bays. Additions of hydrazine to the inspection bay (125 mg/kg) and storage bay (5 mg/kg) decreased the airborne I-131 by a factor greater than seven. The bay purification ion-exchange columns are taken off-line prior to the hydrazine additions, to prevent the removal of ions from the resins. Defect rates at CANDU power stations have been so low since 1972 that the hydrazine treatment has never been repeated. Although now discontinued, the technique is available to CANDU stations if required.

F. Conclusions

(1) Models have been developed to describe the release of fission products from defected fuel into the primary coolant. Analytic expressions are given for the release of iodine and noble gases both during constant reactor operation, and on reactor shutdowns. The theoretical models are in agreement with measured data from in-reactor loop experiments.

(2) Recoil is the dominant mechanism of fission-product release from fuel debris or uranium contamination found on in-core reactor surfaces. This source of activity in the primary heat-transport system can be distinguished from fission products released from fuel-element failures.

(3) Equipment is installed in Canadian CANDU power stations to detect and locate even small defects in failed fuel bundles present in the reactor core.

(4) Proven techniques, based on measuring gaseous and dissolved fission products, radioiodine and delayed neutron precursors, are available to:

   (a) decide if the activity in the reactor coolant originates from tramp uranium or failed fuel,

   (b) estimate the number of failed fuel elements in the reactor core,

   (c) determine the severity of the fuel defects and their probable area of fuel exposed to the coolant (defect size),

   (d) establish the rate of deterioration of defected fuel leading to an optimum time for its removal from the core, and

   (e) predict the release of fission products and radioiodines during reactor power transients.

(5) Identification of failed bundles at the point of transfer between the fuelling machines and the underwater bays may be carried out using dry sipping techniques. In addition, defected bundles can be identified by wet sipping and visual inspection in the irradiated fuel bays using a variety of inspection tools.

G. Acknowledgements

The authors wish to acknowledge the contributions of J.J. Lipsett, R. da Silva, D.D. Semeniuk and the NRX Operations staff to the experimental defect program at CRNL and to acknowledge the cooperation of the Canadian utilities (Ontario Hydro, New Brunswick Power and Hydro-Quebec) for providing feedback on fuel performance. Modelling assistance and helpful discussions were provided by H.E. Sills, E.P. Penswick, J.M. Bunge, F.C. Iglesias, C.E.L. Hunt and C.R. Phillips (of the University of Toronto).

H. References

(1) P.T. Truant and M.R. Floyd, "Canadian Fuel Performance: Ontario Hydro Experience, Past, Present and Future", presented at the International Symposium on Uranium and Electricity, 1988 September 18-21, Saskatoon, Saskatchewan.

(2) D. Barber and D.H. Lister, "Chemistry of the Water Circuits of CANDU Reactors", Water Chemistry and Corrosion Problems in Nuclear Power Plants, International Atomic Energy Agency, Vienna 1983, IAEA-SM-264/15. Also Atomic Energy of Canada Limited, Report AECL-8217.

(3) B.J. Lewis, "Fundamental Aspects of Defective Nuclear Fuel Behaviour and Fission Product Release", J. Nuclear Materials, in press.

(4) R.A. Proebstle, J.H. Davies, T.C. Rowland, D.R. Rutken and J.S. Armijo, "The Mechanism of Defecting of Zircaloy-Clad Fuel Rods by Internal Hydriding", Proc. Joint ANS-CNA Topical Mtg. Commercial Nuclear Fuel Technology Today, Toronto, Canada, 1975.

(5) B. Cox, "Mechanisms of Hydrogen Absorption by Zirconium Alloys", 1984 November, Atomic Energy of Canada Limited, Report AECL-8702.

(6) B.J. Lewis and D.B. Duncan, "Determination of Release Rate from Measured Activity of Depositing Fission Products", Proc. Int. Conf. on CANDU Fuel, ISBN 0-919784-13-5, Chalk River, Canada, 1986 October 6-8, p. 460.

(7) A.H. Booth, "A Suggested Method for Calculating the Diffusion of Radioactive Rare Gas Fission Products from UO_2 Fuel Elements and a Discussion of Proposed In-Reactor Experiments That May be Used to Test its Validity", 1957 September, Atomic Energy of Canada Limited, Report AECL-700.

(8) I.J. Hastings, C.E.L. Hunt and J.J. Lipsett, "Release of Short-Lived Fission Products from UO_2 Fuel: Effects of Operating Conditions", J. Nuclear Materials 130, 1985, page 407.

(9) A.D. Appelhans and J.A. Turnbull, "Measured Release of Radioactive Xenon, Krypton and Iodine from UO_2 During Nuclear Operation and a Comparison with Release Models", Proceedings of the 8th Water Reactor Safety Research Information Meeting, Gaithersburg, Maryland, 1980 October 27-31, US Nuclear Regulatory Commission.

(10) B.J. Lewis, C.R. Phillips and M.J.F. Notley, "A Model for the Release of Radioactive Krypton, Xenon and Iodine from Defective UO_2 Fuel Elements", Nuc. Technology 73, 1986, page 72.

(11) B.J. Lewis, "Fission Product Release from Nuclear Fuel by Recoil and Knockout", J. Nuclear Materials 148, 1987, page 28. Also as Atomic Energy of Canada Limited, Report AECL-9353.

(12) I.J. Hastings, C.E.L. Hunt, J.J. Lipsett and R.D. Delaney, "Short-Lived Fission Product Release from the Surface and Center of Operating UO_2 Fuel", 1984 July, Atomic Energy of Canada Limited, Report AECL-8353.

(13) H. Matzke, "Gas Release Mechanisms in UO_2 - A Critical Review", Radiation Effects 53, 1980, page 219.

(14) D.R. Olander, "Oxidation of UO_2 by High-Pressure Steam", Nuc. Technology 74, 1986, page 215.

(15) B.J. Lewis, D.B. Duncan and C.R. Phillips, "Release of Iodine from Defective Fuel Elements Following Reactor Shutdown", Nuc. Technology 77, 1987, page 303. Also as Atomic Energy of Canada Limited, Report AECL-9368.

(16) G.M. Allison and R.F.J. Robertson, "The Behaviour of Fission Products in Pressurized-Water Systems (A Review of Defect Tests on UO_2 Fuel Elements at Chalk River)", 1961 September, Atomic Energy of Canada Limited, Report AECL-1338.

(17) B.J. Lewis, "Fission Product Release to the Primary Coolant of a Reactor", Proceedings of the Canadian Nuclear Society 6th Annual Conference, Ottawa, Ontario, 1985 June, pages 6-22. Also as Atomic Energy of Canada Limited, Report AECL-8975.

(18) A.M. Manzer, "Transport Mechanisms of Uranium Released to the Coolant from Fuel Defects", Proceedings of the International Conference on CANDU Fuel, Chalk River, Canada, 1986 October 6-8.

(19) D.R. McCracken and M.R. Floyd, "Studies of Activity Transport and Fission Product Behaviour in Water Cooled Nuclear Generating Stations and the Consequences for Defected Fuel Removal", presented at the Cdn. Nucl. Soc. "Water Chemistry and Material Performance Conference", Toronto, Ontario, 1986 October.

(20) A.M. Manzer, unpublished report, 1982 September.

(21) A.M. Manzer, R.W. Sancton and N. Macici, "Canadian CANDU 6 Perspective on Fuel Integrity Performance Indicators", 1987 September, Atomic Energy of Canada Limited, Report AECL-9602.

(22) R.D. MacDonald, J.J. Lipsett, E.E. Perez and P.K. Kos, "Purposely Defected UO_2-Zircaloy Fuel Elements Irradiated in Pressurized Light Water at Linear Powers of 55 kW/m", 1983 May, Atomic Energy of Canada Limited, Report AECL-7751.

(23) A.M. Manzer, "In-Core Assessment of Defective Fuel in CANDU 600 Reactors", Presentation at the IAEA Specialists Meeting on Post-Irradiation Examination and Experience, Tokyo, Japan, 1984 November.

(24) G.M. Allison and H.K. Rae, "The Release of Fission Gases and Iodine from Defected UO_2 Fuel Elements of Different Lengths", 1965 June, Atomic Energy of Canada Limited, Report AECL-2206.

(25) S. Jacobi, K. Lety and G. Schmety, "Release and Detection of Fission Products from Defected Fuel Pins", Nuclear Engineering and Design 44, 1977, pages 125 to 135.

(26) A.M. Manzer and R.W. Sancton, "Detection of Defective Fuel in an Operating CANDU 600 MW(e) Reactor", Presentation at the ANS Conference on Fission Product Behaviour and Source Term Research, Snowbird, Utah, 1984 July.

(27) R.D. MacDonald and J.J. Lipsett, "The Behaviour of Defected Zircaloy-Clad UO_2 Fuel Elements with Graphite Coatings Between Fuel and Sheath Irradiated at Linear Powers of 48 kW/m in Pressurized Water", 1980 May, Atomic Energy of Canada Limited, Report AECL-6787.

(28) J. Judah, "Defective Fuel Location by Dry Sipping: Experience at Bruce NGS-A During the 1984 Fuel Defect Excursion", Proc. Int. Conf. on CANDU Fuel, ISBN 0-919784-13-5, Chalk River, Canada, 1986 October 6-8, p. 470.

(29) P.T. Truant and R.D. MacDonald, "Documentation and Post-Irradiation Examination of Canadian Nuclear Fuel", 1985 September, Atomic Energy of Canada Limited, Report AECL-8904.

(30) C.R. Frost, "Operating Experience with Ontario Hydro's Spent Fuel Bays", Proceedings of the Irradiated Fuel Storage: Operating Experience and Development Program Meeting, Toronto, Canada, 1984 October 17-18, page 51.

TABLE 1
SUMMARY OF EXPERIMENTS WITH SINGLE DEFECTED FUEL ELEMENTS OF CRNL

1.1 Artificially-defected fuel

Experiment (Element)	Test Description	Defect Description	Defect Size (mm^2) Initial	Defect Size (mm^2) Final	Linear Power (kW/m)	Burnup (MW.h/kgU) Initial	Burnup (MW.h/kgU) Final	Defect residence time (effective full power days)	Irradiation date
FDO-681									
Phase 1 (RPL)	Irradiation of	Single hole (1.3 mm)*	1.3	1.3	49	140**	158	15	1975 July 24 to Aug 10
Phase 2 (LFZ)	elements with	Single hole (1.2 mm)*	1.1	1.1	48	0	20	24	1975 Aug 10 to Sep 23
Phase 3 (RPP)	drilled hole(s)	Two holes (1.3 & 0.4 mm)*	1.5	1.5	47	140**	173	35	1975 Oct 8 to Nov 16
FDO-687									
Phase 1 (RPR)	Irradiation of	Single hole (2.0 mm)*	3.1	3.1	55	43**	85	40	1976 Mar 13 to Apr 25
Phase 2 (NSZ)	elements with	Slit (10 mm x 0.6 mm)*	6.0	6.0	58	0	28	26	1976 Apr 30 to May 26
Phase 3 (RPR)	drilled holes(s) or single slit	Three holes+	7.2	7.2	54	85	90	4	1976 June 10 to June 14
FFO-101 (A3M)	Irradiation of an element with a drilled hole	Single hole (1.0 mm)*	0.8	0.8	39	0	45	47	1979 Jan 3 to Mar 5
FFO-103 (A3N)	Irradiation of an element with 23 slits	23 slits in a helical pattern along sheath (ea.slit 36 mm x 0.3 mm)	272	1490++	48	0	18	15	1981 May 30 to June 14

* Located at element midlength. ** Irradiated intact to this burnup.
\+ Two additional 1.6 mm holes were drilled, one at each end of the element.
++ Slits enlarged during irradiation due to fuel expansion from UO_2 oxidation. Defect size estimated from post-irradiation examination.

TABLE 1
CONTINUED

1.2 Naturally-defected fuel

Experiment (Element)	Test Description	Defect Description	Defect size (mm^2) Initial	Defect size (mm^2) Final	Linear Power (kW/m)	Burnup (MW.h/kgU) Initial	Burnup (MW.h/kgU) Final	Defect residence time (effective full power days)	Irradiation date
FFO-102-2 (A7E)	Re-irradiation of an element with through-wall hydriding at high power	Cracked hydride blisters at one end of element	11	300+	67	37	67	19	1981 Mar 17 to Apr 5
FFO-102-3 (A7A)	Re-irradiation of an element with incipient sheath hydriding at low power	Six randomly located, small hydride cracks	-*	-	23	68	130	110	1981 July 30 to 1982 Nov 5
FFO-104 (A2F)	Power ramp failure by stress-corrosion cracking	Nine randomly located, small hydride cracks	0.0**	45+	58	255	278	16	1981 May 6 to May 24
FFO-110 and	Power-cycling of an element	Six randomly located, small	-	-	14-26	130	140	18	1983 Mar 23 to Apr 10
FFO-109 (A7A)	with through-wall hydriding	hydride cracks	-	<1+	22-38	140	155	19	1983 Apr 27 to May 10

* Element A7A initially had a porous end plug fabrication flaw of about 0.4 microns.
** Element A2F was initially intact, but failed in-reactor following a power ramp.
\+ Defect sizes estimated from post-irradiation examinations.

TABLE 2
FUEL-ELEMENT DESIGN

	Fuel-Element Classification*	
	Class I	Class II
Fuel description		
Sintered UO_2 density (Mg/m^3)	10.7	10.7
Enrichment (wt % ^{235}U in uranium)	4.5	5.0
Pellet diameter (mm)	13.7	12.1
Pellet length (mm)	19.0	16.5
Pellet end dishing	one end	both ends
Land width (mm)	0.56	0.46
Depth (mm)	0.64	0.23
Fuel stack length (mm)**	179.0	477.0
Sheath description		
Material	Zircaloy-4	Zircaloy-4
Outside diameter (mm)	15.2	13.1
Wall thickness (mm)	0.71	0.43
Clearances		
Diametral (mm)	0.10	0.10
Axial (mm)	1.0	2.2

* Class I elements include: RPL,LFZ,RPP,RPR and NSZ. Class II elements include: A3M,A3N,A7E,A7A and A2F.

** Elements LFZ and NSZ, and A3N, had slightly smaller fuel stack lengths of 168 and 470 mm, respectively.

TABLE 3
LOOP OPERATIONAL PARAMETERS

Thermal flux (axially averaged)	$5.5 \times 10^{13} n/cm^2.s$
Temperature	240 - 260°C
Pressurized water	7.7 - 10.5 MPa
Flow rate	0.6 - 1.1 kg/s
Recirculation time	105 s
Coolant pH (LiOH controlled)	10 - 11
Hydrogen content	5 - 20 mL/kg
Graphite filters	6 µm
Coolant volume	0.15 m^3

TABLE 4
EXPONENTIAL DEPENDENCE OF R/B ON THE DECAY CONSTANT

	Experiment									
	FDO-681			FDO-687			FFO-102		FFO-103	FFO-104
	1	2	3	1	2	3	2	3		
Defect classification and size, mm^2	hole 1.3	hole 1.1	2 holes 1.5	hole 3.1	slit 6.0	3 holes 7.2	hydride 11-200	hydride -	23 slits 300-1500	hydride ~45
Exponential dependence										
Iodine	-1.83	-1.53	-0.90	-1.23	-1.29	-1.15	-1.26	-0.98	-0.64	-0.71
Krypton + ^{138}Xe	-0.96	-1.13	-0.87	-1.07	-0.95	-0.79	-1.15	-1.05	-0.64	-1.08
Xenon*	-0.77	-0.99	-0.59	-0.70	-0.78	-0.68	-0.72	-1.02	-0.65	-0.48

* Xe-135 is plotted against an effective decay constant to account for neutron absorption effects.

TABLE 5
FACTORS FOR PRECURSOR DIFFUSION

	Krypton			Xenon				Iodine				
	85m	87	88	133	133m	135	138	131	132	133	134	135
H'	1.9	1.7	1.1	1.2	1.4	3.0	1.0	1.0	11.7	1.1	2.1	1.0

TABLE 6
SUMMARY OF SLOPES FROM LOG R/B VERSUS LOG λ PLOTS

Defect Size	UO_2 Exposure* (mm^2)	Dependence**	
		Iodine	Noble Gas
Large	300-1500	-0.5	-0.5
Moderate	11 - 200	-1.0	-1.0
Small	≤1	-1.5	-1.0

* Range of defect size investigated (see Table 4)
** Exponential dependence of R/B on λ.

CANDU FUEL AND FUELLING DATA

REACTOR		PICKERING	BRUCE	CANDU-6
NUMBER OF ELEMENTS PER BUNDLE		28	37	37
ELEMENTS				
OUTSIDE DIAMETER	mm	15.19	13.08	13.08
MIN. CLADDING THICKNESS	mm	0.38	0.38	0.38
BUNDLES				
LENGTH	mm	495,3	495.3	496.3
MAXIMUM DIAMETER	mm	102.49	102.49	102.49
NUMBER PER CHANNEL		12	13	12
NUMBER IN CORE		12	12	12
OPERATING CONDITIONS				
NOMINAL INLET PRESSURE	MPa	9.6	10.2	
NOM. MAX. HEAT RATING	kW/m	4.2	4.43	
MAXIMUM LINEAR ELEMENT POWER	kW/m	52.8	55.67	
MAX. SURFACE HEAT FLUX	kW/m	1120.	1354.7	
FUELLING DIRECTION		With Flow	Against Flow	

FUEL BUNDLE CROSS SECTIONS

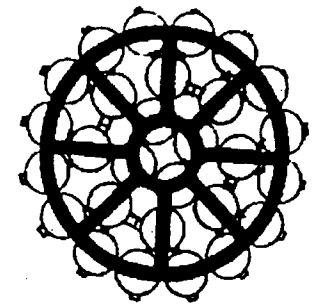

PICKERING

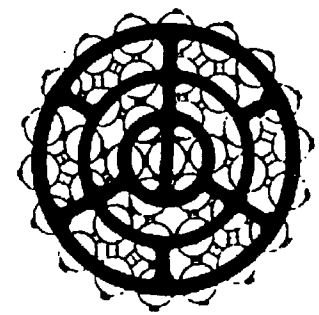

BRUCE

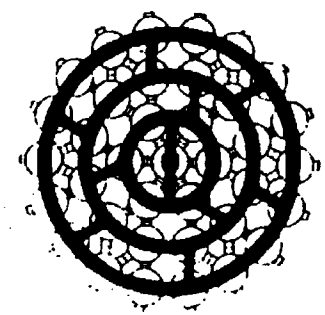

CANDU-6

FIGURE 1 CANDU FUEL ELEMENT & BUNDLE PARAMETERS

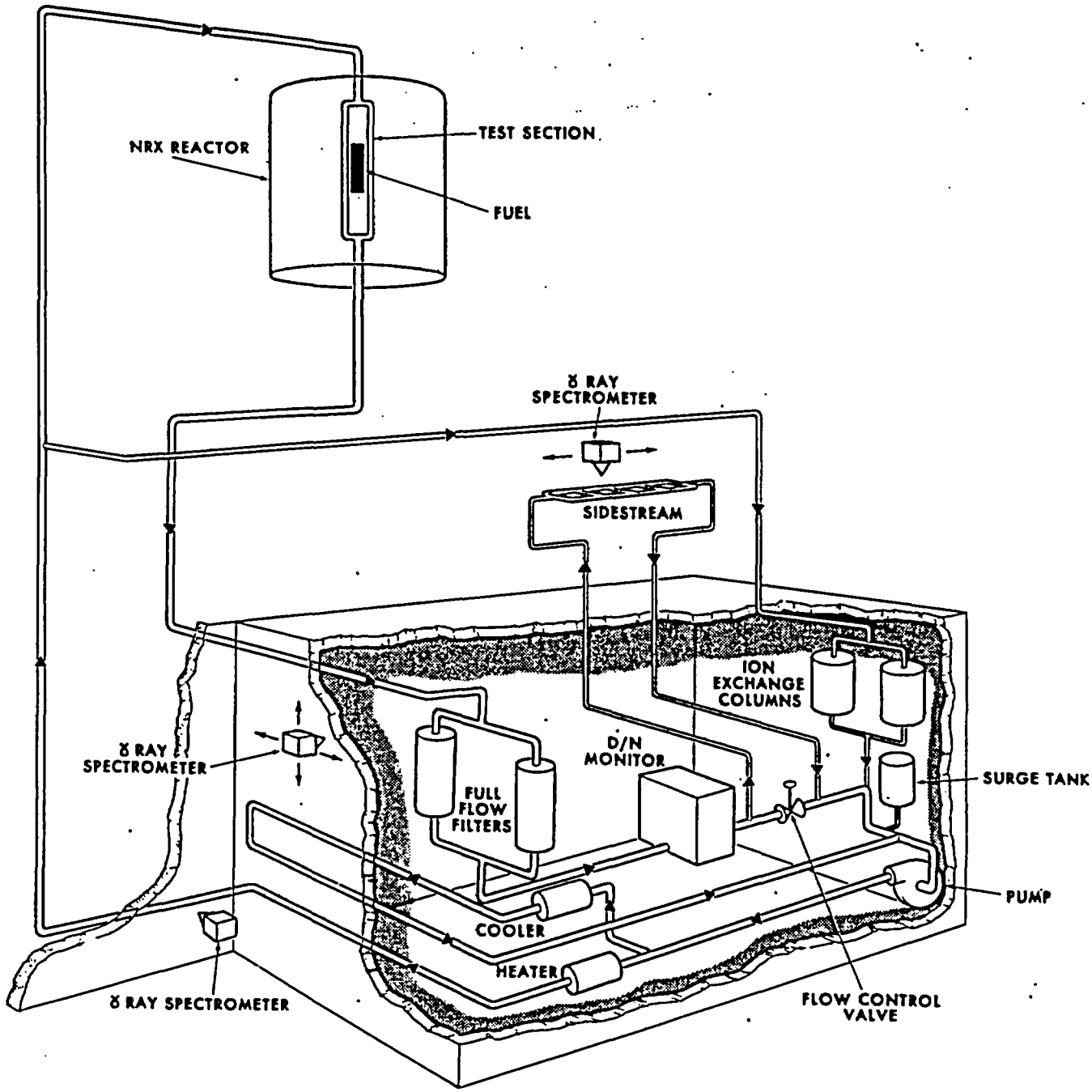

FIGURE 2 SCHEMATIC DIAGRAM OF THE X-2 DEFECT LOOP

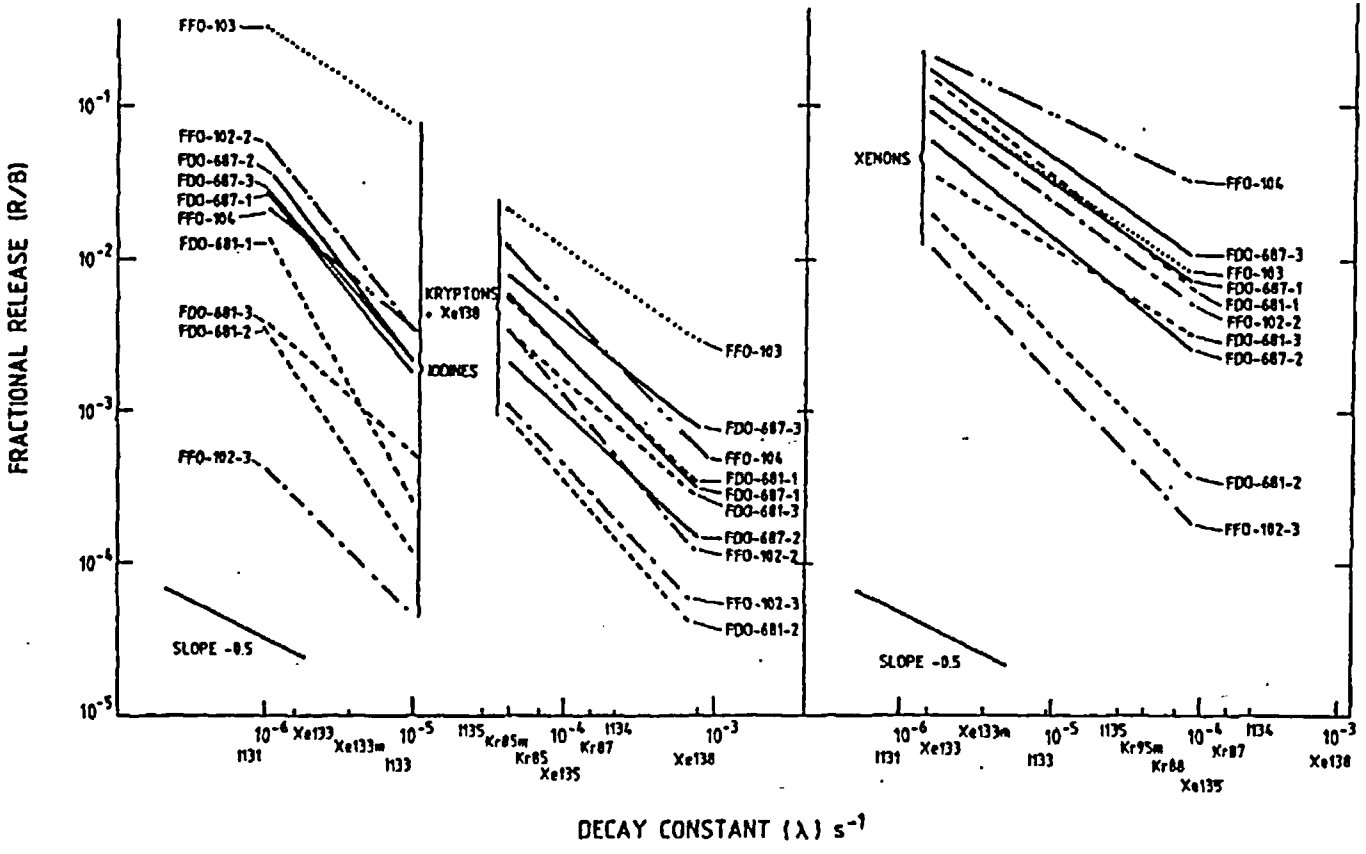

FIGURE 3 Steady-state R/B versus decay constant plot for noble gases and radioiodine releases from defect experiments at Chalk River

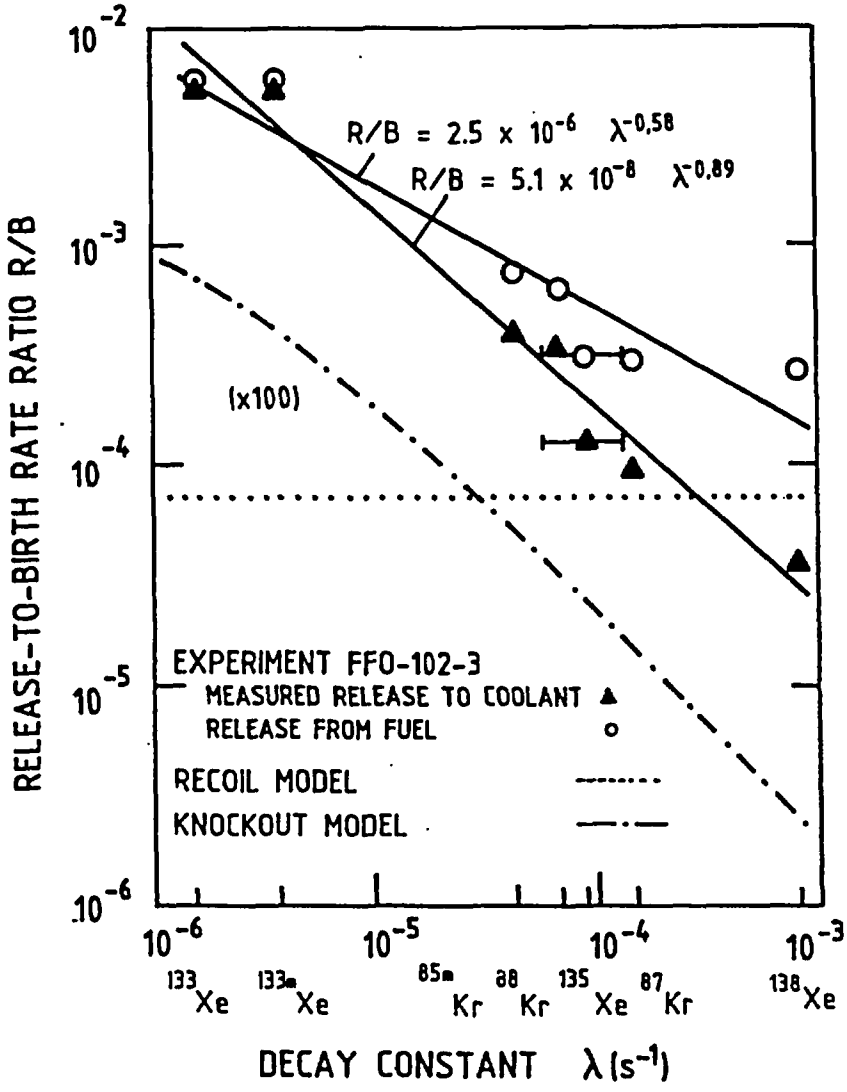

FIGURE 4 . **Comparison of the estimates of recoil and knockout release with measured data for experiment FFO-102-3 (Note: The knockout releases are actually a factor of 100 less than that shown above)**

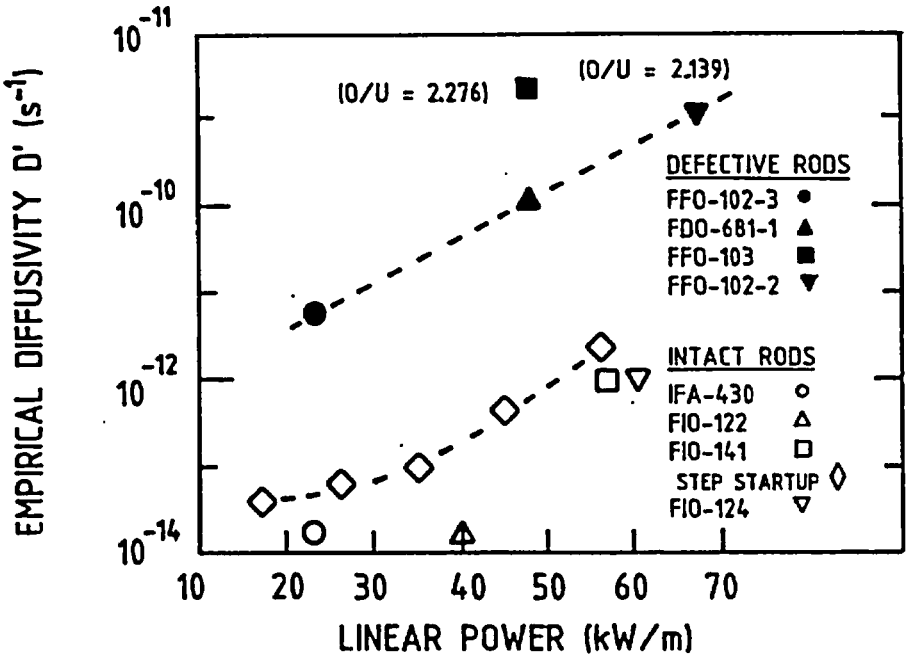

FIGURE 5 Correlation of empirical diffusion coefficients (for noble gas in UO_2) versus linear power for both intact and defected fuel elements

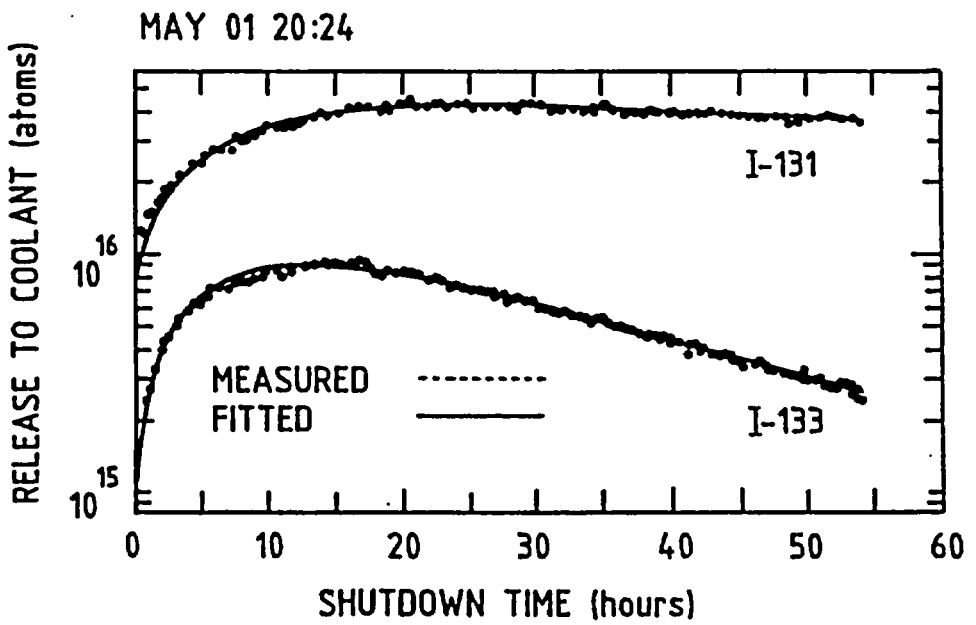

FIGURE 6 Fitting the iodine release model to data for I-131 and I-133 from experiment FFO-109-2

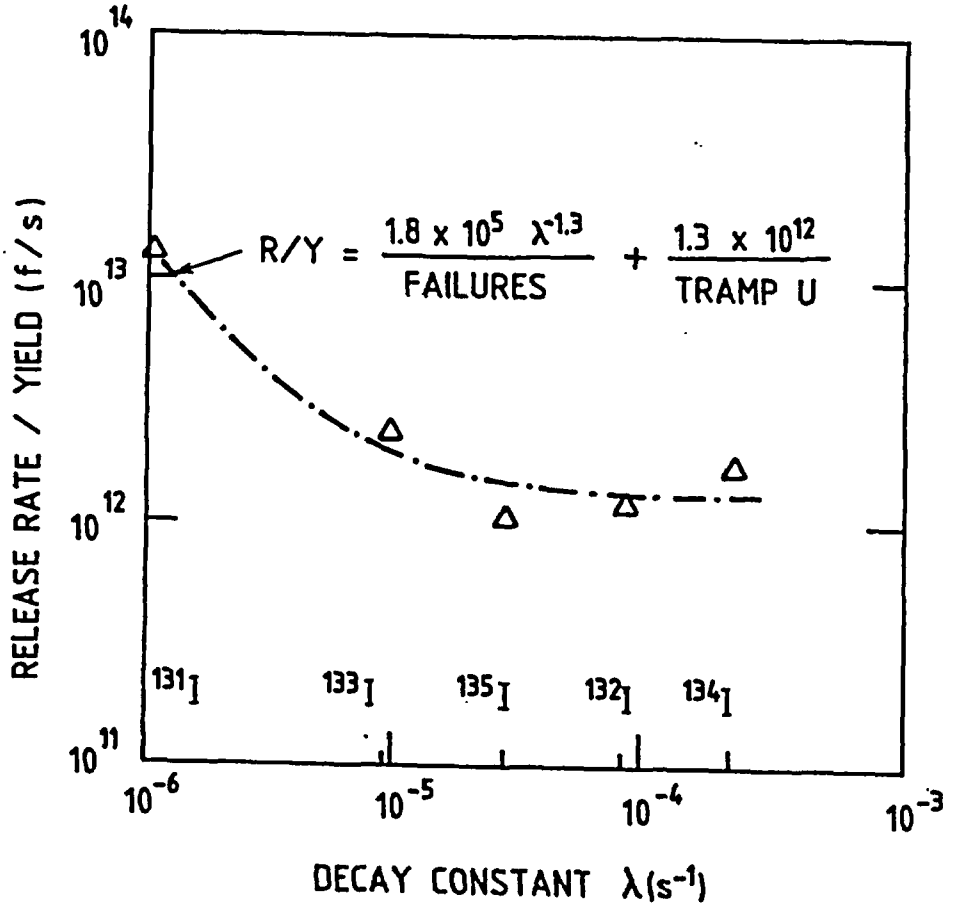

FIGURE 7 **Fitting the fission-product release model to release data for the Point Lepreau reactor. Data sample 86/10/19. The release data have been corrected for Pu-239 production assuming a burnup of 100 MW.h/kgU**

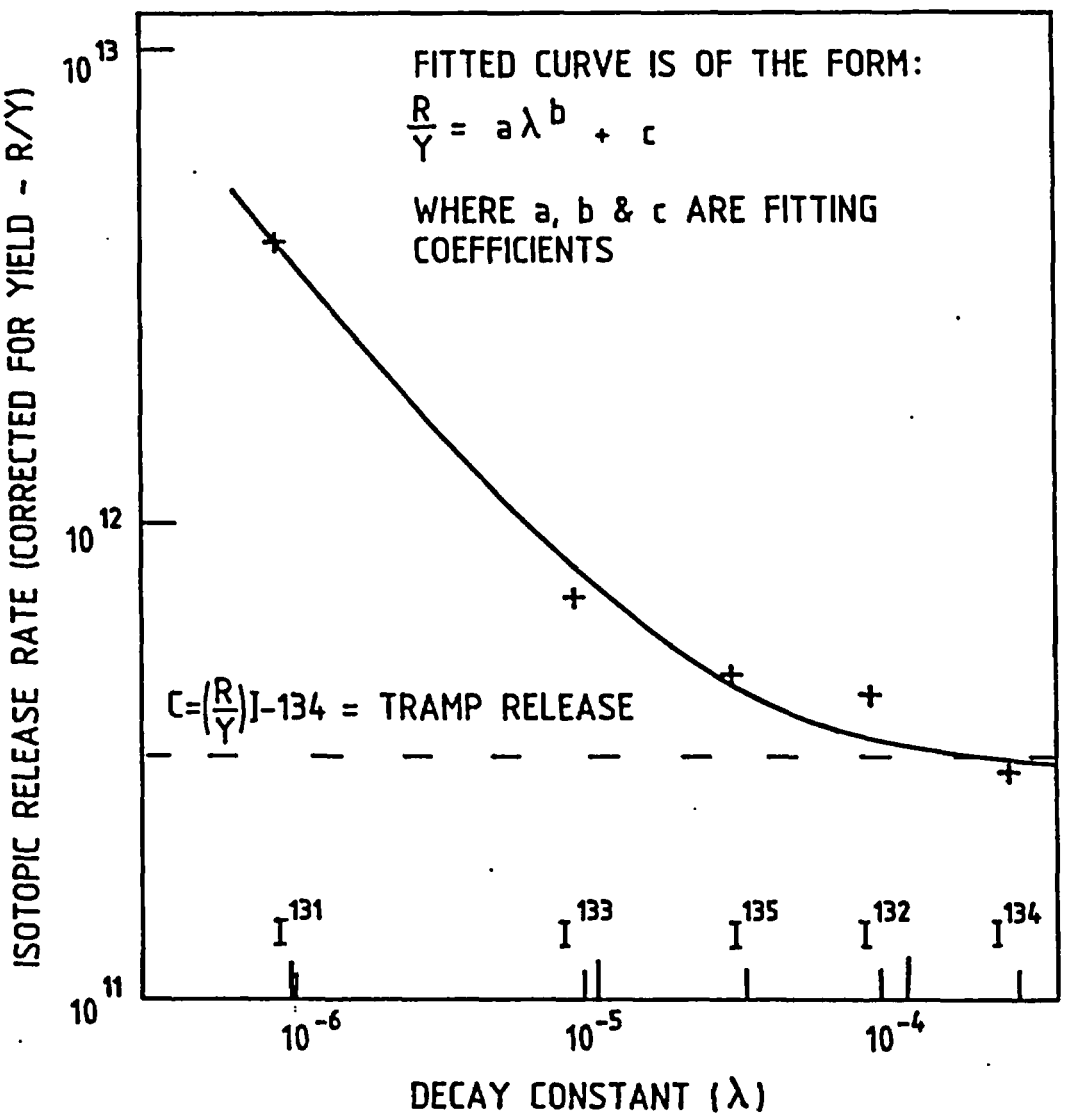

FIGURE 8 Estimation of release from tramp uranium from the Bruce B unit 6 reactor

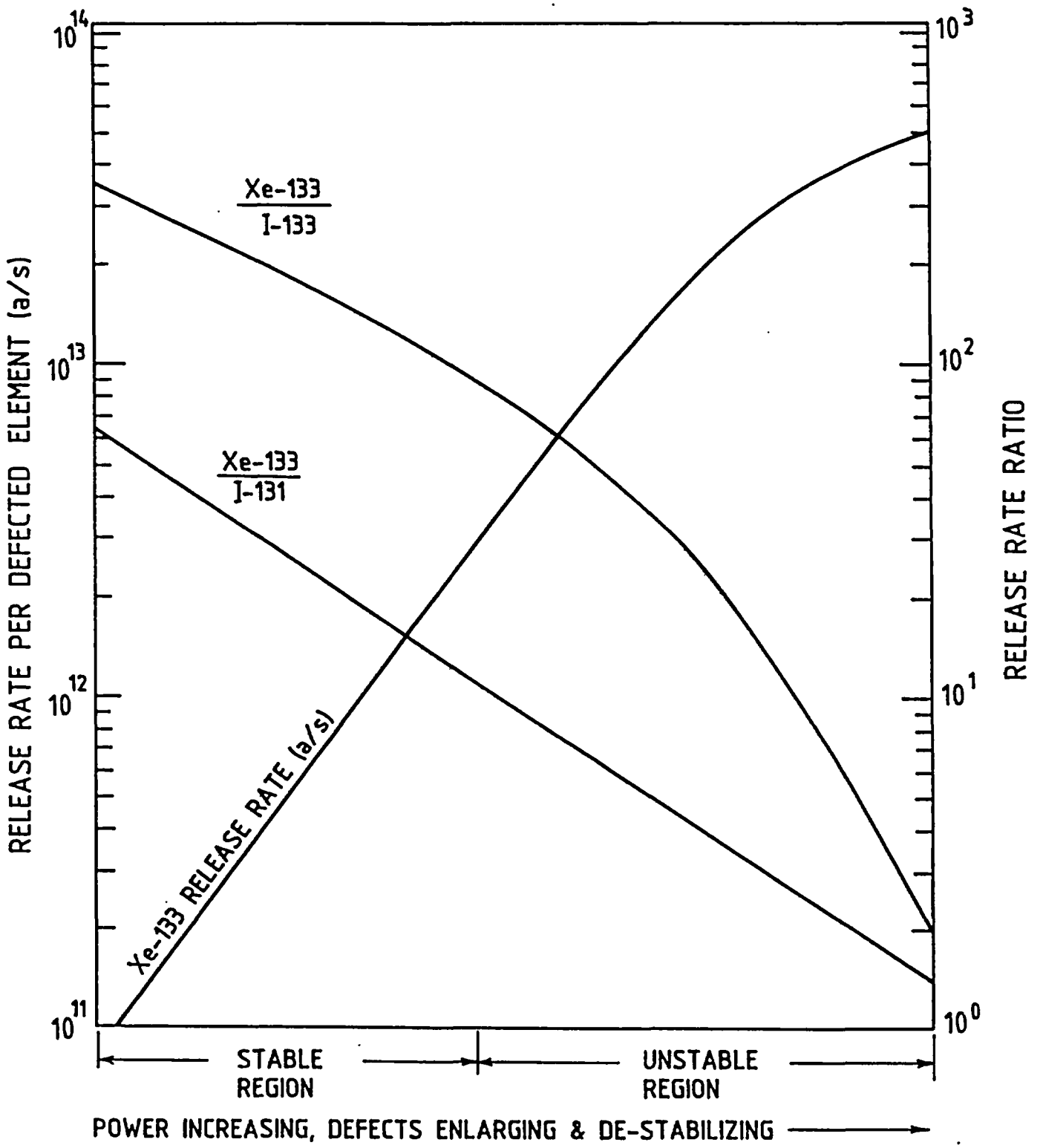

FIGURE 9 **Determination of the predominant defect type and estimation of the number of defected elements**

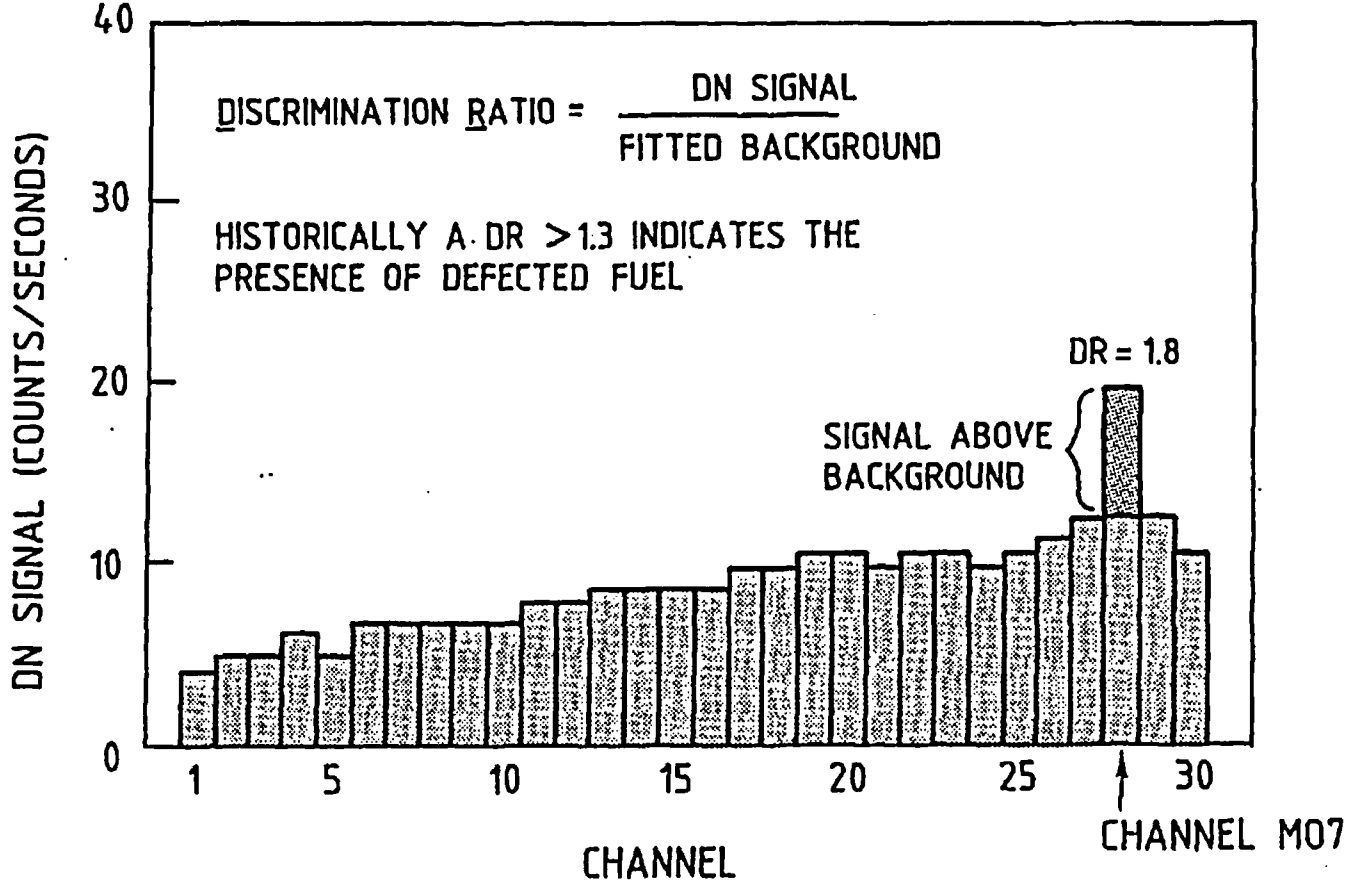

FIGURE 10 **Delayed neutron signals from a row of 30 channels, one of which contains defected fuel in the Bruce B Unit 6 reactor.**

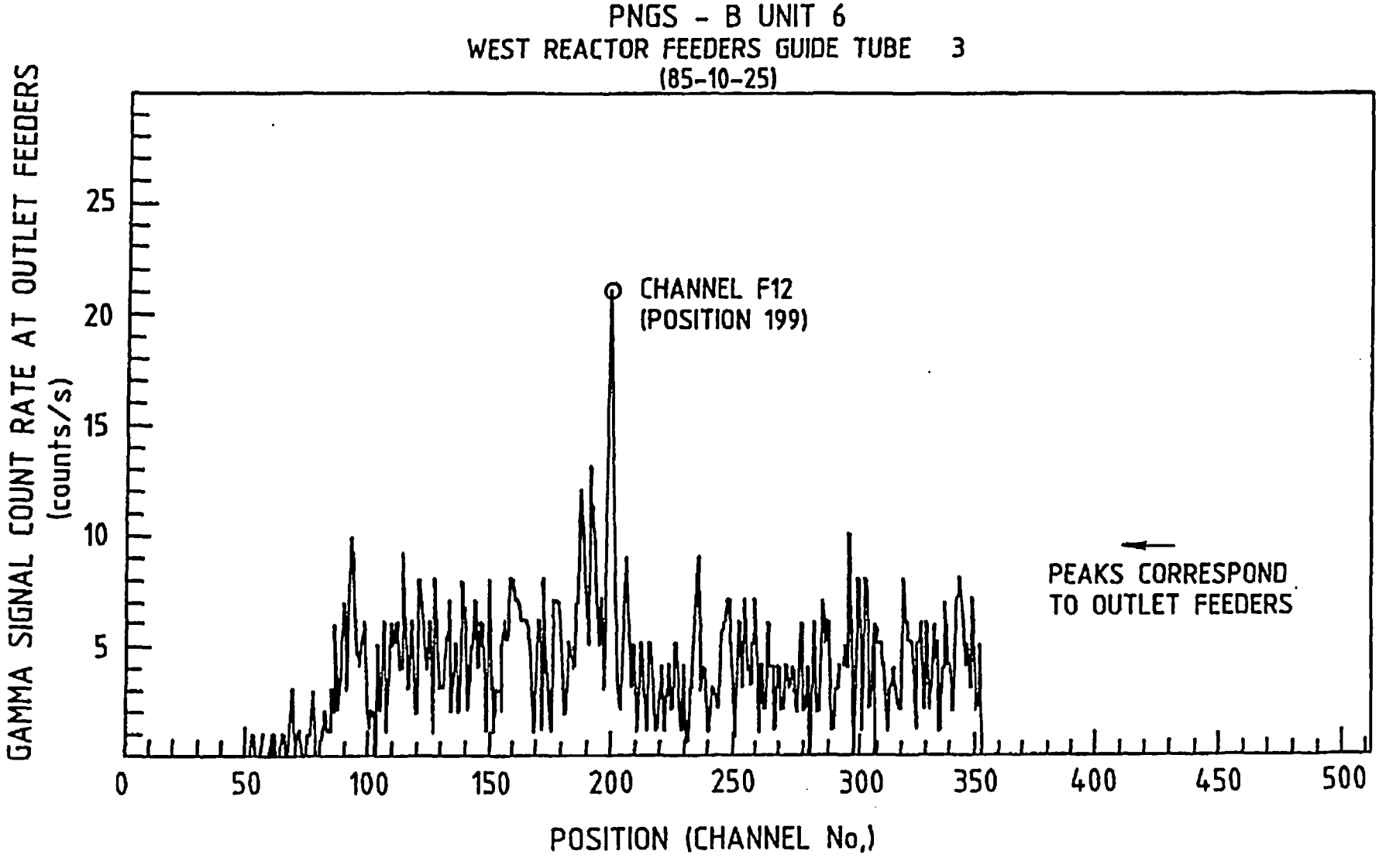

FIGURE 11 Typical scan data from a feeder scanner

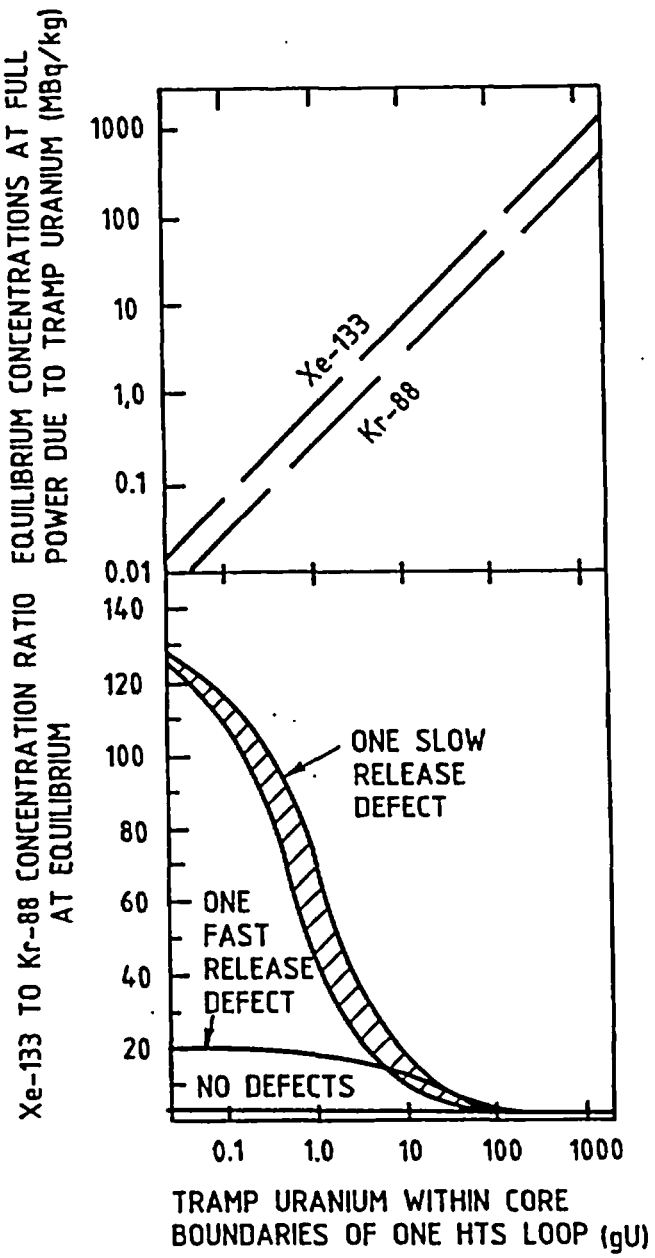

FIGURE 12 **Graphs showing the effects of tramp uranium on:**

(A) the equilibrium activity concentrations of Xe-133 and Kr-88, and

(B) Xe-133 to Kr-88 concentration ratio

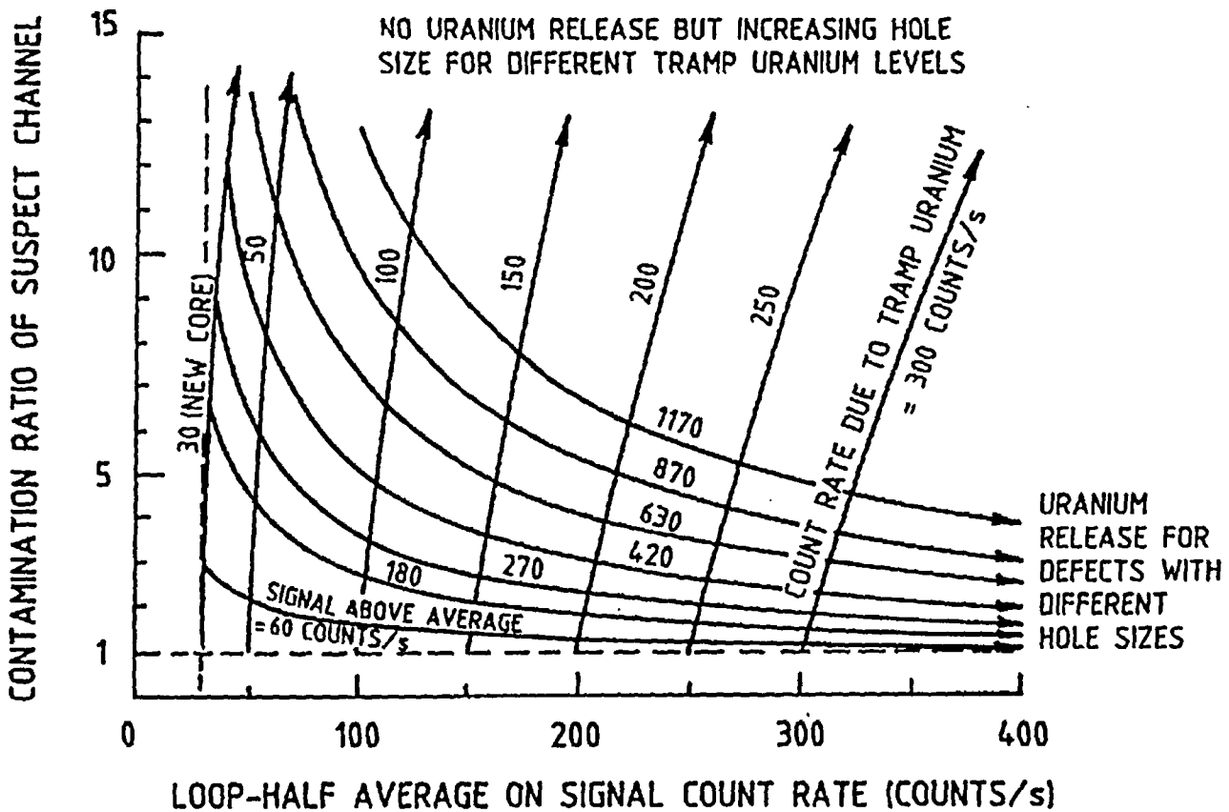

FIGURE 13 Predicted discrimination ratio behaviour for a defected fuel element deteriorating by: (A) increasing defect hole size or (B) uranium release

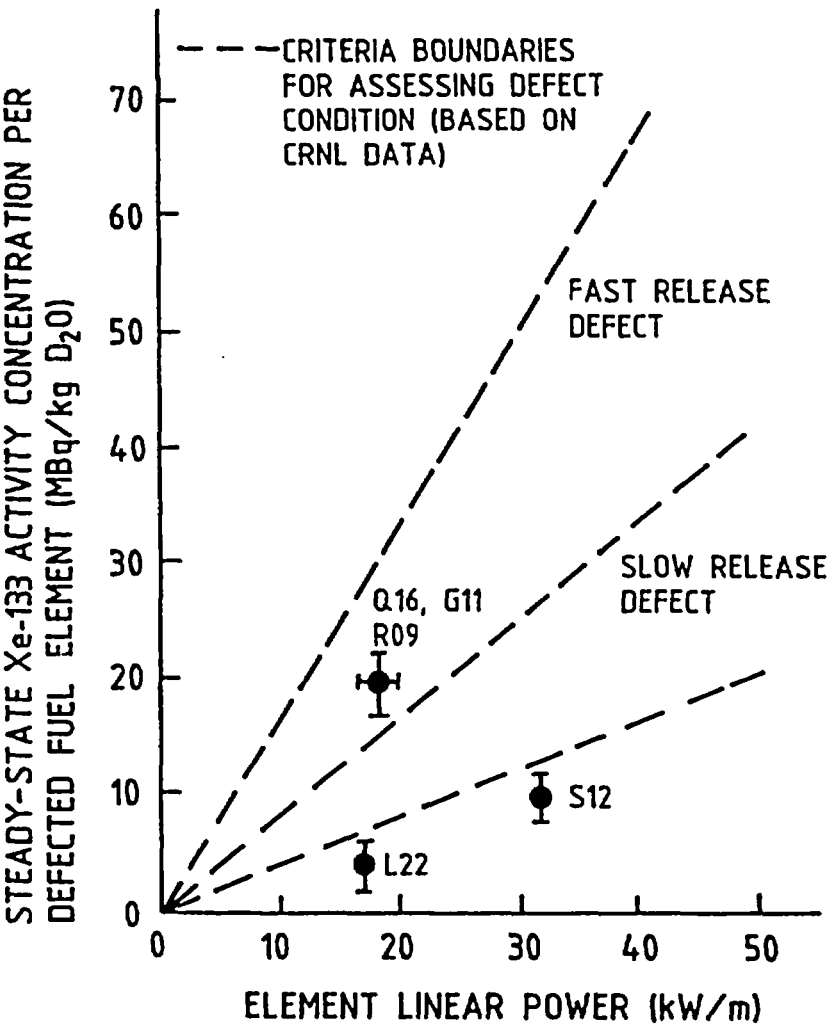

FIGURE 14 **Steady-state Xe-133 activity releases from fuel defects in the Point Lepreau reactor**

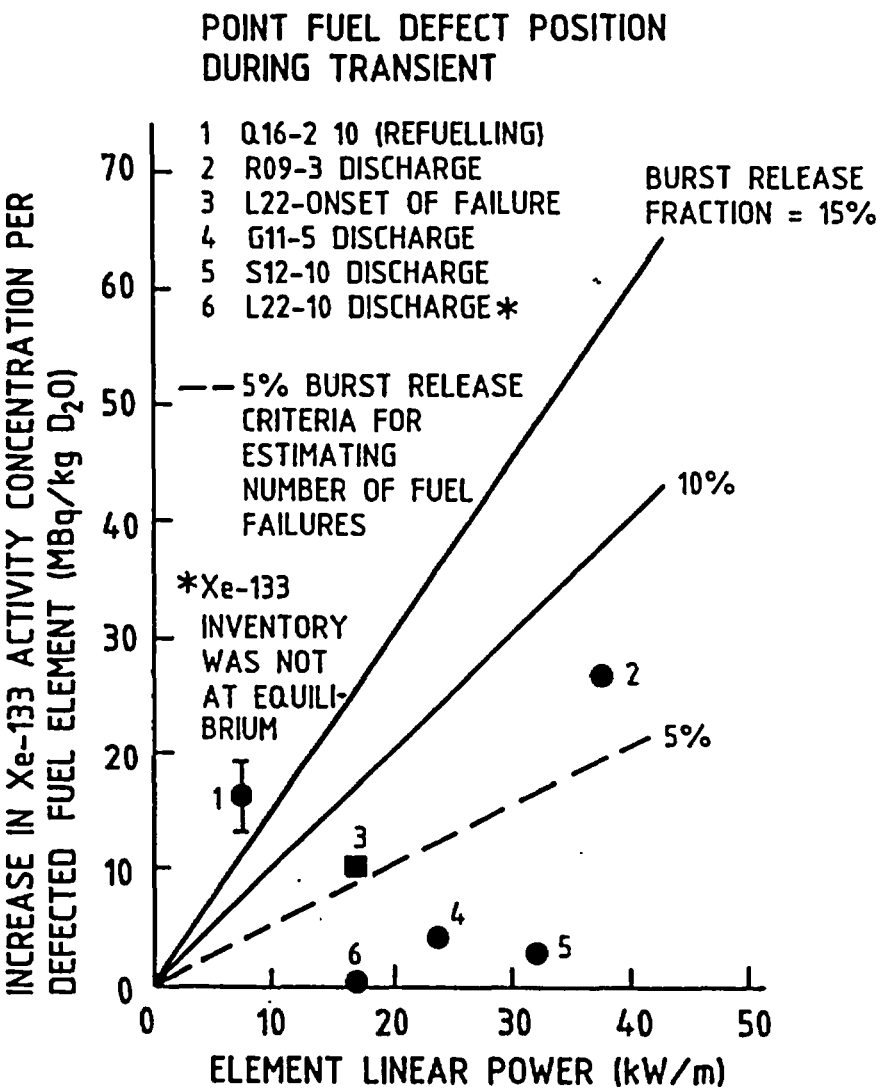

FIGURE 15 **Transient Xe-133 activity releases from fuel defects in the Point Lepreau reactor**

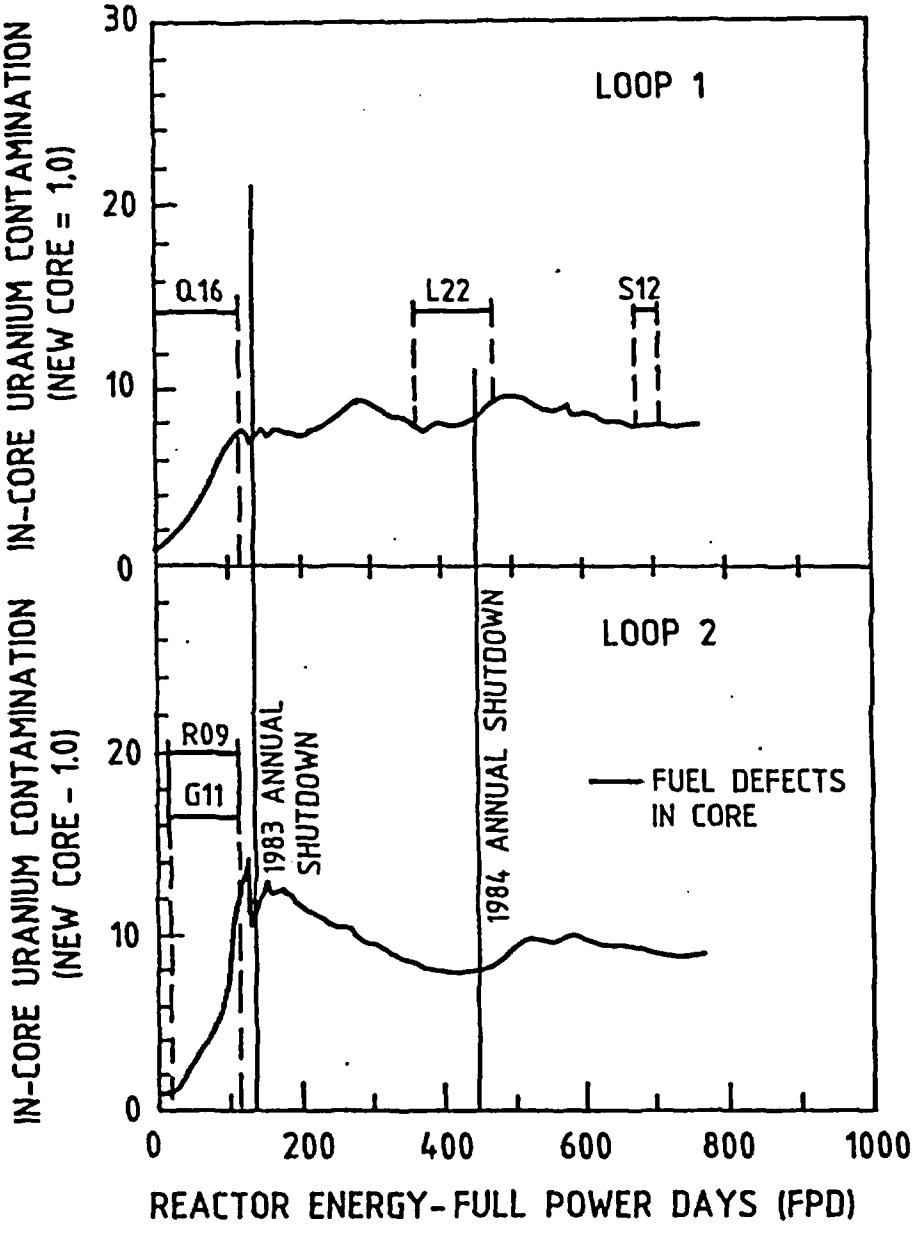

FIGURE 16 **In-core uranium contamination level for loops 1 and 2 of the Point Lepreau reactor**

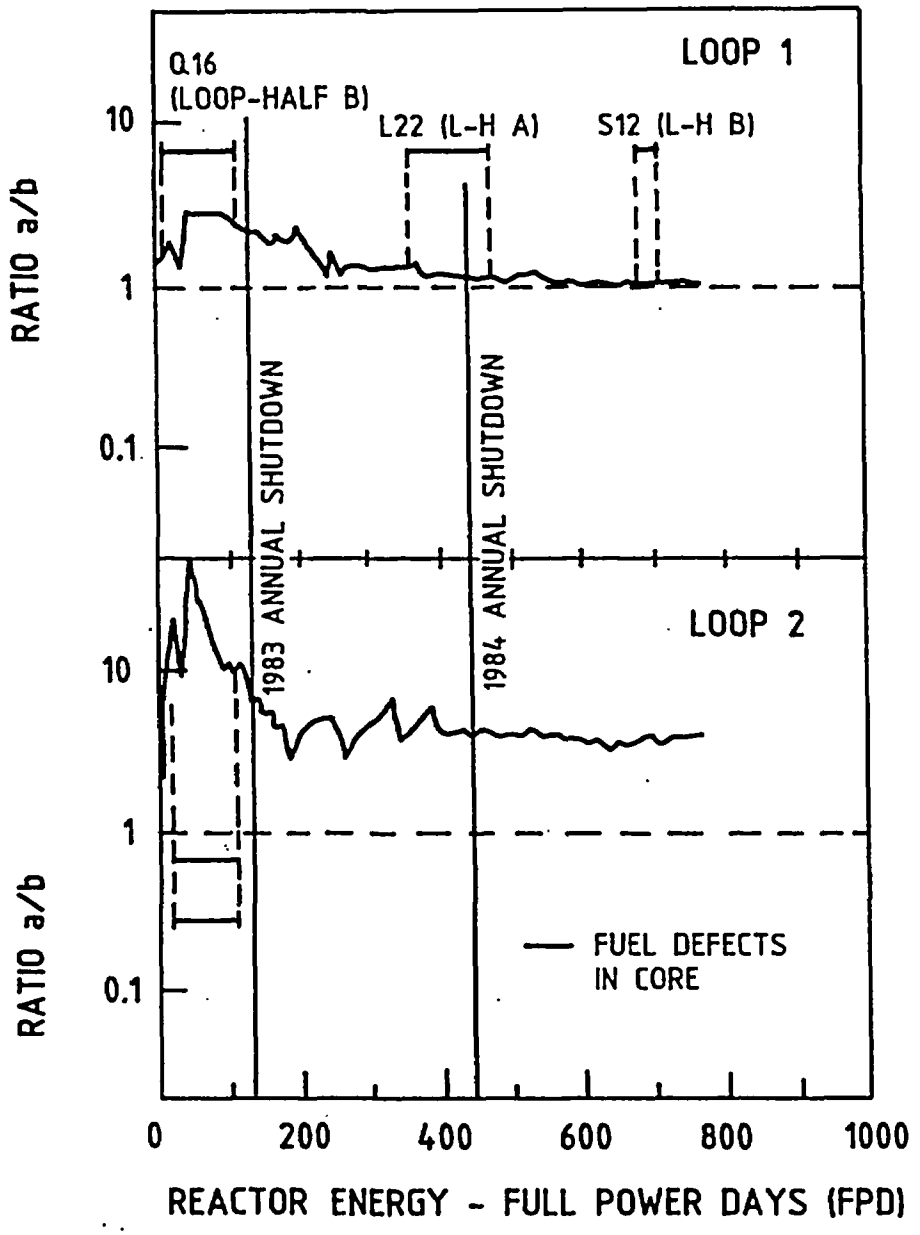

FIGURE 17 **Ratio of in-core uranium contamination between loop halves for loops 1 and 2 of the Point Lepreau reactor**

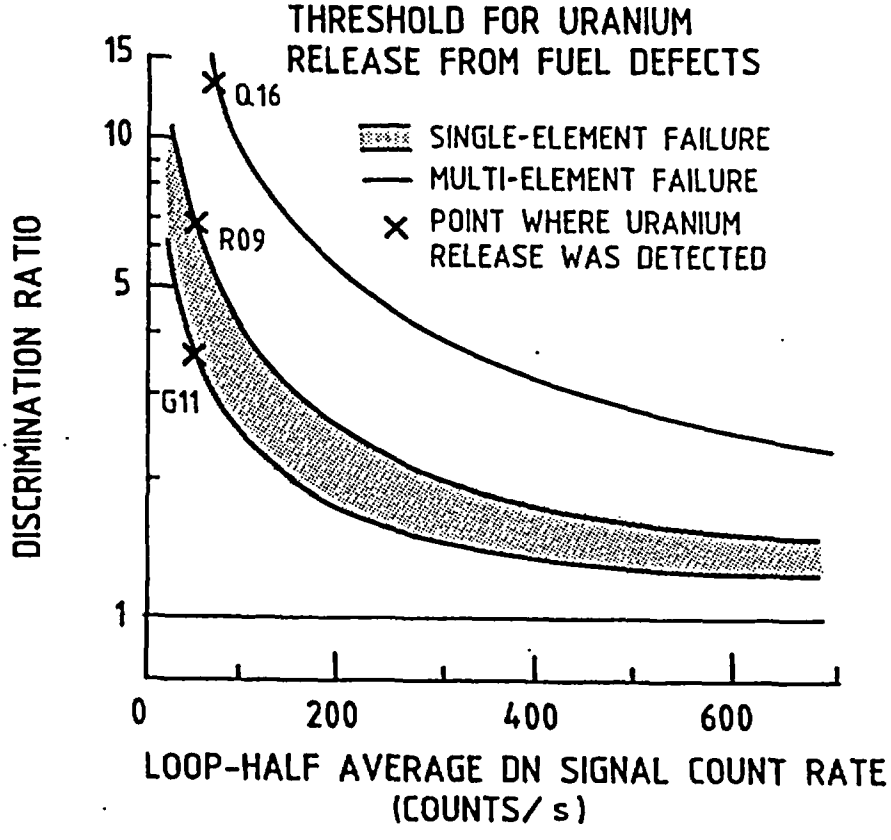

FIGURE 18 Thresholds for uranium release for single and multiple fuel-element failures

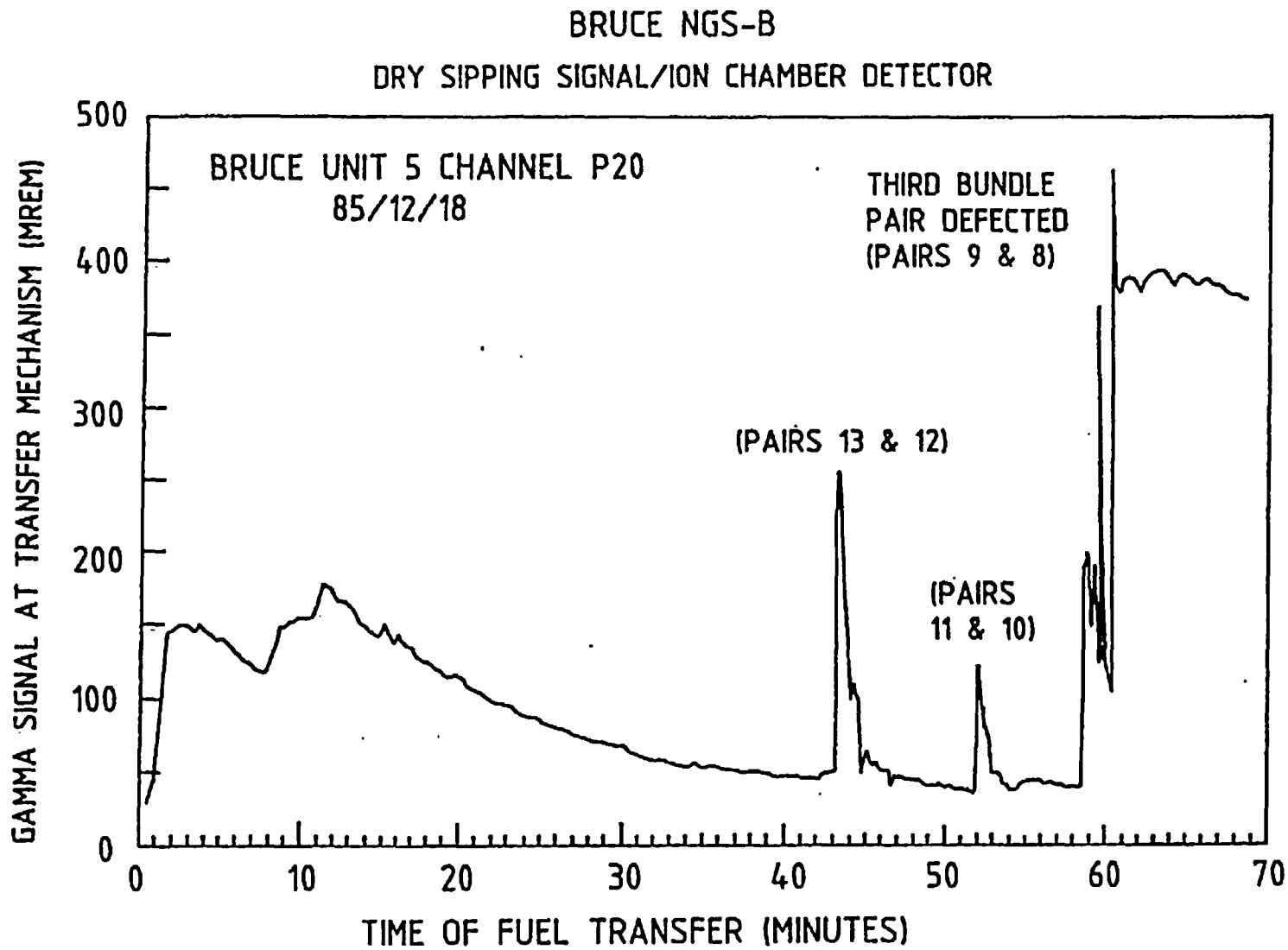

FIGURE 19 **Typical dry sipping data from the fuel transfer mechanism of a power station**

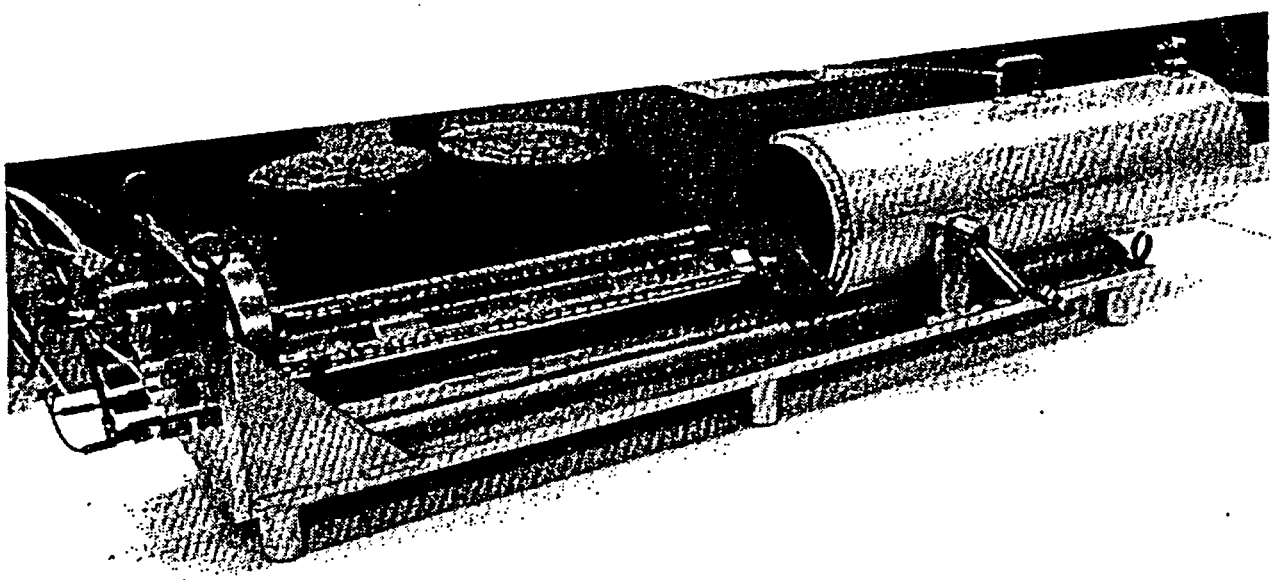

FIGURE 20 Underwater canister of the defected fuel identification apparatus

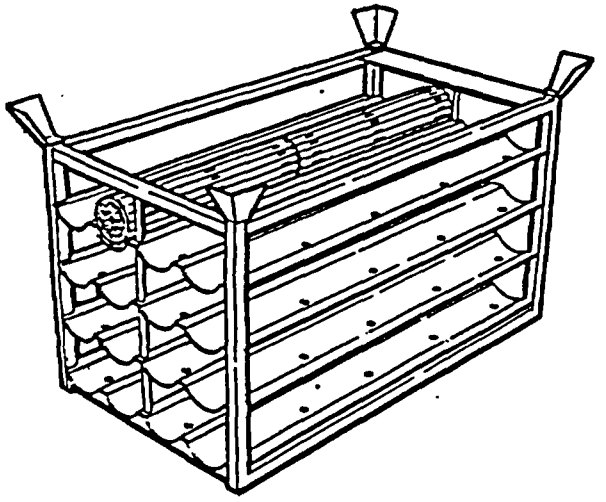

PICKERING GS FUEL STORAGE BASKET
(32 BUNDLE CAPACITY, STORAGE
DENSITY = 1393 kg U/m^3)

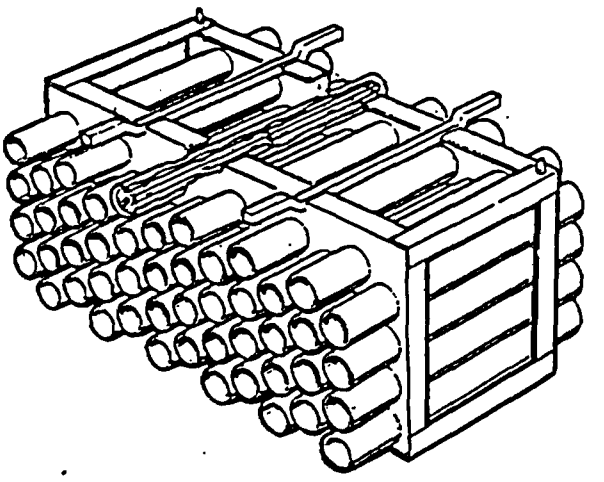

SHIPPING AND STORAGE MODULE
(96 BUNDLE CAPACITY, STORAGE
DENSITY = 2189 kg U/m^3)

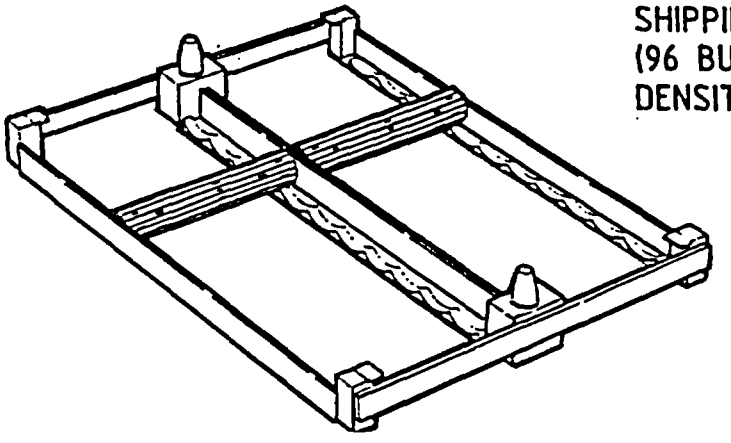

BRUCE GS IRRADIATED FUEL
STORAGE TRAY
(20 BUNDLE CAPACITY, STORAGE
DENSITY = 1683 kg U/m^3)

FIGURE 21 **Ontario Hydro irradiated fuel storage containers**

ISSN 0067-0367

To identify individual documents in the series we have assigned an AECL- number to each.

Please refer to the AECL- number when requesting additional copies of this document

from

Scientific Document Distribution Office
Atomic Energy of Canada Limited
Chalk River, Ontario, Canada
K0J 1J0

Price: B

ISSN 0067-0367

Pour identifier les rapports individuels faisant partie de cette série nous avons assigné un numéro AECL- à chacun.

Veuillez faire mention du numéro AECL- si vous demandez d'autres exemplaires de ce rapport

au

Service de Distribution des Documents Officiels
Énergie atomique du Canada limitée
Chalk River, Ontario, Canada
K0J 1J0

Prix: B

591-90